BLIND COLLISION RESOLUTION FOR WIRELESS MULTIPLE ACCESS USING INDEPENDENT COMPONENT ANALYSIS

by

Barış Özgül

B.Sc., Electrical and Electronics Engineering, Boğaziçi University, 1998

Submitted to the Institute for Graduate Studies in
Science and Engineering in partial fulfillment of
the requirements for the degree of
Master of Science
in
Electrical and Electronics Engineering

Boğaziçi University

2002

BLIND COLLISION RESOLUTION FOR WIRELESS MULTIPLE ACCESS USING INDEPENDENT COMPONENT ANALYSIS

APPROVED BY:

Prof. Hakan Deliç ....
(Thesis Supervisor)

Assoc. Prof. Cem Ersoy ....

Assoc. Prof. Ayşın Ertüzün ....

DATE OF APPROVAL: 24.06.2002

ACKNOWLEDGEMENTS

Başarımdaki en büyük payın sahibi olan *annem Sabriye, babam Ali Riza* ve *ağabeyim Alper Özgül'e*; çalışmalar sırasında ilgisini hiçbir zaman eksik etmeyen tez danışmanım *Prof. Hakan Deliç*'e ve bu süreç boyunca bana her zaman destek olan sevgili *Ülgen Satıoğlu*'na teşekkürlerimi ve saygılarımı sunuyorum.

ABSTRACT

BLIND COLLISION RESOLUTION FOR WIRELESS MULTIPLE ACCESS USING INDEPENDENT COMPONENT ANALYSIS

In wireless random access networks, packet collision is an important medium access problem for the packet radio environment. Simple protocols such as the *slotted ALOHA* do not provide an efficient solution to the collision problem since they generally suffer from a severe throughput penalty and the underutilization of the channel resources. Thus, signal separation techniques used in signal processing can be employed to improve the throughput and delay performance of the system. *Network-assisted diversity multiple access* (NDMA) and *blind network-assisted diversity multiple access* (BNDMA) are two such techniques. User specific ID sequences are necessary to be inserted to the transmitted data packets to resolve the collision by NDMA. BNDMA does not need this requirement, and collision is resolved by using *parallel factor* (PARAFAC) analysis. In this thesis, *independent component analysis* (ICA) is integrated into the multiple access mechanism to provide a significant improvement in terms of system throughput and the transmission delay. Performance comparisons with NDMA and BNDMA are furnished. The number of unresolved packet retransmissions is controlled by the base station and can be decreased through spatial diversity.

ÖZET

TELSİZ ÇOKLU ERİŞİM İÇİN BAĞIMSIZ BİLEŞEN ANALİZİ KULLANARAK GÖZÜ KAPALI ÇARPIŞMA ÇÖZÜNÜRLÜĞÜ

Telsiz rasgele erişim şebekelerinde birden fazla kullanıcının aynı anda arama yapması durumunda kullanıcıların veri paketleri çarpışır. Alıcı tarafından bu paketlerin ayrıştırılması için kullanılan *dilimli ALOHA* gibi klasik yöntemlerin, yeniden iletim açısından oldukça uzun zaman harcadıklarından dolayı, zayıf bir üretilen iş ve gecikme başarımı sergiledikleri bilinmektedir. Bu durum, sinyal işleme uygulamalarında kullanılan sinyal ayrıştırma yöntemlerinin yukarıda bahsedilen çarpışma sorununun çözümü için kullanılmasını gündeme getirmiştir. Bunun sonucu olarak *şebeke çeşitlemeli çoklu erişim* (ŞÇÇE) ve *gözü-kapalı şebeke çeşitlemeli çoklu erişim* (GŞÇÇE) gibi uygulamalar denenmiş ve çok daha iyi başarım sergilemişlerdir. Bu yöntemlerde çarpışma sonrasında veri paketlerinin yeniden iletimi belirli bir sayıda olup, kesinlikle rasgele bir ozellik göstermemektedir. ŞÇÇE çarpışma çözünürlüğünü her kullanıcının veri paketine sadece o kullanıcıya özgü bir kimlik kodu ekleyerek sağlamaktadır. GŞÇÇE ise bu işi, *Paralel Çarpan Analizi* kullanarak, gözü kapalı bir biçimde halletmektedir. Bu çalışmada bir başka gözü kapalı kaynak ayırma yöntemi olan *bağımsız bileşen analizi* (BBA) kullanılarak çarpışma çözünürlüğü yüksek bir üretilen iş ve gecikme başarımıyla sağlanmaktadır. Ayrıca, BBA başarımı ŞÇÇE ve GŞÇÇE yöntemlerininkiyle karşılaştırılmaktadır. BBA'nin da ihtiyaç duyduğu yeniden iletim sayısı belirli olup, uzam çeşitlemesi kullanılarak bu sayı daha da aza indirilebilmektedir.

TABLE OF CONTENTS

LIST OF FIGURES

LIST OF SYMBOLS/ABBREVIATIONS

$\lceil \, \rceil$	Integer ceiling operator
$\{ \, \}$	Epoch length operator
A	Arithmetic mean function
$\mathbf{A}_{L\times K}$	Channel mixing matrix
b	Binomial mass function
D	Mean delay
$\overline{D}$	Average delay
f	Fading coefficent
$f_D(d)$	Delay pdf
g	Antenna gain
G	Geometric mean function
H	Epoch length
H_r	Relevant epoch length
H_{ir}	Irrelevant epoch length
$\mathbf{I}$	Identity matrix
J	Number of users in the system
K	Number of collided users
L	Number of observations at the base station
M	Number of receiver antennas at the base station
N	Packet length
R	Number of transmissions
$\mathbf{S}_{K\times N}$	Independent data packet matrix
$\mathbf{V}_{L\times N}$	Additive Gaussian noise matrix
$\mathbf{Y}_{L\times N}$	Observed data matrix
α	Fading amplitude
ϕ	Fading phase
φ	Transmitter phase
λ	Packet arrival rate

λ_{max}	Maximum packet arrival rate
λ_T	Throughput
δ	Delta function
$\mathbf{\Sigma}$	Noise covariance matrix
σ_v^2	Noise variance

AIC	Akaike information criterion
AMPS	Advanced mobile phone services
BNDMA	Blind network diversity multiple access
BPSK	Binary phase shift keying
BS	Base station
BSS	Blind source separation
CDMA	Code division multiple access
CRC	Cyclic redundancy check
CSMA	Carrier sensing multiple access
ETACS	Extended total access communication system
EVD	Eigenvalue decomposition
FDMA	Frequency division multiple access
GSM	Global system for mobile
ICA	Independent component analysis
i.i.d.	Independent and identically distributed
ITC	Information theoretical criteria
MAC	Medium access control
min	minimum function
NDMA	Network diversity multiple access
PARAFAC	Parallel factor analysis
pdf	Probability density function
PRMA	Packet reservation multiple access
RAA	Random access algorithm
rank	Rank function
real	Real function

sgn	Signum function
SNR	Signal to noise ratio
SVD	Singular value decomposition
TC-RAA	Two-cell random access algorithm
TDMA	Time division multiple access

1. INTRODUCTION

Random access algorithms (RAAs) are well-suited for various applications in wireless communications since these algorithms are implemented independently by each user, result in low delays when the traffic is bursty, and are insensitive to changing user population. For instance, RAAs are used for mobile-to-base station signaling in second generation cellular telephony (*random access channel* (RACH) in GSM system uses a slotted-ALOHA access scheme [1], and TIA IS-95 standard uses pure ALOHA [2]), or access coordination between voice and data in the third generation universal mobile telecommunication system [1]. Moreover, RAAs are widely used to control the packet data traffic in the local area networks such as Ethernet [3]. There is also a different approach to use RAAs as a multiple access scheme for bursty data sources depending on the increasing demand for data and multimedia communication in slotted wireless networks.

Contrary to bursty data, voice communication requires a *circuit-switched, constant bit rate* service for each user. *Frequency division multiple access* (FDMA) and *time division multiple access* (TDMA) were/are widely used multiple access methods for voice services in wireless networks. FDMA, as a multiple access scheme, was used in first generation cellular systems such as AMPS and ETACS [1]. However, since FDMA provides low user capacity, continuous transmission and fixed channels which can be regarded as wasted sources when idle, it is not suitable to accommodate bursty users. TDMA is widely used in second generation wireless networks. However, TDMA has also some drawbacks due to its fixed channel allocation strategy. When the system is highly loaded, system throughput is also high since the majority of the time slots are used for transmission. However, most of the slots stay idle under low traffic, which is not well-suited for multiplexing *variable bit rate* data sources, so resulting in low throughput performance. Thus, previously mentioned qualities of RAAs such as handling bursty traffic with low delays and being insensitive to changing user population come up with the idea of using RAAs as a multiple access scheme for bursty data sources, which are expected to be simpler to implement than *code division multiple* *access* (CDMA) [1]. For instance, in [4], the slotted ALOHA RAA is proposed to have better performance than CDMA and TDMA under some simplified conditions about the propagation changes. In addition, *packet reservation multiple access* (PRMA), which uses random access techniques for the channel slot assignment, is shown to have similar performance to CDMA if signal powers of the transmitted packets are sufficiently high [5].

Slotted ALOHA [6], as a well-known RAA, is suitable for bursty users, but suffers from weak throughput and delay performances depending on packet collisions among different users. This is because the ALOHA-type protocols discard all collided packets in the event of a collision and require the retransmission of them after waiting for a random number of time slots, until all the packets are received individually without any collision. The maximum throughput that slotted ALOHA can provide is 0.368, which is extremely low [1]. Moreover, slotted ALOHA is an unstable RAA and the throughput goes to zero as the number of users increase. The collision multiplicity needs to be known to stabilize slotted ALOHA which makes this algorithm more complex [3]. The performance of slotted ALOHA can be improved by using *carrier sensing multiple access* (CSMA) [1, 3] to prevent collisions. In CSMA, a user can determine whether other users are transmitting after a very small propagation and detection delay relative to a packet transmission time. The detection time is the duration necessary for a user to determine whether or not some other user is currently transmitting. However, this approach is not very reliable in wireless channels because of obstacles such as fading and shadowing. There are also some other previously developed RAAs in [7, 8, 9, 10, 11] which depend on the following idealized conditions:

- The transmission channel is slotted and noiseless. Each packet has a constant one-slot duration. Collisions are always detected, but the information in the collided packets is lost. Thus, retransmissions of collided packets are necessary.
- There is a noiseless feedback channel which informs the users immediately at the end of each slot whether that slot was idle, or contained one packet (successful transmission), or contained more than one packet (collision).
- Propagation delays are negligible and it can be assumed that the feedback infor-

mation for one slot can be used to determine who should transmit in the following slot.

- There are infinite number of users in the system, and the cumulative input traffic is *Poisson*.

The sharpest upper bound for throughput provided among these algorithms is 0.587, as stated in [12]. However, the performance of these RAAs in a mobile environment varies. The slotted ALOHA RAA has been studied in the presence of multipath fading and shadowing in [13, 14], and does not have a desirable performance. However, there are some stable RAAs with better performance. One of them is the *two-cell random access algorithm* (TC-RAA) [9]. A modified version of TC-RAA that takes advantage of packet capture out of a collision was proposed in [15]. Packet capture depends on the ability of receiving one packet correctly out of all the colliding packets if its signal power is sufficiently strong. Otherwise, all collided packets are lost. This property obviously has a positive impact on the throughput and delay performance. Later, the *mobile radio window random access algorithm* (MRW-RAA), which augments TC-RAA with antenna diversity capability was investigated in a mobile radio environment with capture, fading, shadowing, and path loss in [16]. In MRW-RAA, the capture effect and the diversity techniques help to resolve the collision in a shorter duration. The results in [16] indicate that MRW-RAA is the far superior choice over slotted ALOHA. The maximum throughput of MRW-RAA, analytically derived for various diversity schemes under Rayleigh and Rician fading, shadowing, and path-loss, is as high as 0.7 depending on the channel parameter values [16].

Despite the enhancements mentioned above, random access techniques still do not provide a high throughput and delay performance for wireless data communications. The RAAs concentrate on decreasing the number of retransmissions, but they simply discard the collided packets rather than processing the received data. Even the algorithms which benefit from packet capture, do not have the capability of retrieving two or more collided packets from the received data. However, signal separation techniques used in signal processing applications can be employed on the received data for collision resolution to improve the throughput and delay performance of the system.

Network Diversity Multiple Access (NDMA) [17, 18] and *Blind Network Diversity Multiple Access* (BNDMA) [18, 19] are two such multiple access methods which have been developed so far. NDMA needs user specific orthogonal ID sequences to be inserted as a prefixes to the transmitted data packets to detect the number of collided packets (collision multiplicity) and to resolve the collision. No channel slot is wasted by using NDMA so that K transmissions (or $K-1$ retransmissions) are sufficient to detect the multiplicity and provide the resolution of a K-packet collision. If antenna diversity is available at the base station (BS), even fewer retransmissions less than $K-1$ may suffice. However, due to the orthogonality assumption, longer ID sequences are necessary as the population size increases. This situation results in an increasing overhead which has a negative impact on the bandwidth that carries the packet payload. Therefore, if packet lengths are fixed, the maximum throughput reduces as the population of the system increases. BNDMA, as a blind method, does not need user specific ID sequences. In BNDMA, collision multiplicity is determined by using the *rank test method* [19] and collision resolution is provided by employing PARAFAC analysis [19, 18, 20, 21, 22]. BNDMA spends one more slot to detect the collision multiplicity so that $K+1$ number of transmissions (or K retransmissions) are necessary to detect the collision multiplicity and provide the resolution in case of a K-packet collision. Similar to NDMA, fewer retransmissions may be adequate for BNDMA to resolve the collision if the antenna diversity is available at BS. In case of a noiseless environment, there is no throughput upper bound for BNDMA as the number of users in the system increases [19]. In both NDMA and BNDMA, since the number of retransmissions is determined and controlled by BS, and the collided packets are not simply discarded, high throughput and delay performance is obtained. More detailed descriptions of NDMA and BNDMA will be given in Chapter 2.

In this thesis, we develop a new collision detection and resolution method for the medium access control (MAC) layer by employing *Independent Component Analysis* (ICA) which is assisted with blind collision multiplicity detection. ICA is a statistical method which can represent a set of random variables as a linear combination of a set of independent component variables [23, 24, 25, 26, 27, 28]. One of the popular applications of ICA is *blind source separation* (BSS) [29, 30, 31, 32], where ICA resolves a source mixing problem with no side information. Therefore, our proposed ICA-based multiple access method is fully blind. Similar to NDMA and BNDMA, retransmissions are controlled by BS and the collided packets are not discarded. If the collision multiplicity is known, ICA resolves a K-fold collision in K number of transmissions ($K-1$ retransmissions). Two more retransmissions are necessary to detect the collision multiplicity. Similarly, if ICA is assisted by spatial diversity at the BS, the number of retransmissions necessary for collision resolution reduces even more. If there are M antennas at the BS and it is known that K packets are collided, only $\lceil K/M \rceil - 1$ retransmissions are adequate for ICA to separate each individual user's packet ($\lceil\rceil$ stands for the integer ceiling operator). Therefore, the throughput and delay performance of the wireless system is improved significantly by using ICA, and there is no analytical throughput upper bound as the number of users in the system increases in case of a noiseless environment. In the thesis, ICA-based method is compared to NDMA and BNDMA, and several advantages of ICA are established depending on wireless environment, signaling model, throughput, and system delay.

1.1. Outline and Contributions

In the following chapters, a signaling model which expresses the packet collisions as a source mixing problem is established. Channel effects of multipath fading and additive Gaussian noise are taken into account. After giving a brief summary about NDMA and BNDMA, the properties and requirements of ICA are described and the ICA-based collision resolution algorithm is described. Next, the details of the proposed multiple access protocol are furnished and an analytical framework is referred to express its performance in terms of system throughput and mean transmission delay. In addition, experimental results for the performance depending on the simulations run for several finite *signal to noise ratio* (SNR) values are given.

There are several advantages of the ICA-based multiple access protocol over other proposed methods as will be collaborated in later chapters.

- No need for the user specific orthogonal ID sequences.

- Employed in faster fading channels.
- Insensitive to the transmitter and receiver phase differences.
- Better delay performance in the presence of spatial diversity.

2. BACKGROUND

2.1. The Signaling Model for the Collision Problem

The collided data observed at the receiver antenna of the BS can be considered as the sum of the packets of each user transmitted through different paths. If the channel fading is flat and varies slowly enough during the time slot that packets are transmitted, it can be assumed that each packet transmitted from a different path is multiplied by a different constant path gain. If antenna arrays are available at the BS, the received data at each antenna are also multiplied by a different antenna gain. Assume that R is the necessary number of transmissions to detect and resolve K collided packets. Since a different output is observed at each of M antennas after every transmission, the total number of observations at the BS is $L = R \times M$. As a result, the received data at the BS after R transmissions can be represented by the following equation.

$$\mathbf{Y}_{L\times N} = \mathbf{A}_{L\times K}\mathbf{S}_{K\times N} + \mathbf{V}_{L\times N}. \tag{2.1}$$

The matrix $\mathbf{S}_{K\times N}$ contains the N-bit data packets transmitted by the independent users, where it is assumed that each independent packet is *stationary* and *binary*-distributed with zero mean and unit variance. The bits of each independent packet are assumed to be drawn from a *binary phase shift keying* (BPSK) constellation. The matrix $\mathbf{Y}_{L\times N}$ contains the collided baseband data. Each row of the matrix $\mathbf{Y}_{L\times N}$ corresponds to one of the discrete time packets observed at the BS after matched filtering and sampling at the bit rate. The mixing matrix $\mathbf{A}_{L\times K}$ includes the fading coefficients and the antenna gains. Finally, the matrix $\mathbf{V}_{L\times N}$ includes the white Gaussian noise added to the collided data. Equation (2.1) can also be represented as follows.

$$\underbrace{\begin{bmatrix} \mathbf{Y}_1 \\ \vdots \\ \mathbf{Y}_M \end{bmatrix}}_{\mathbf{Y}_{L\times N}} = \underbrace{\begin{bmatrix} \mathbf{A}_1 \\ \vdots \\ \mathbf{A}_M \end{bmatrix}}_{\mathbf{A}_{L\times K}} \mathbf{S}_{K\times N} + \underbrace{\begin{bmatrix} \mathbf{V}_1 \\ \vdots \\ \mathbf{V}_M \end{bmatrix}}_{\mathbf{V}_{L\times N}} \tag{2.2}$$

where,

- $\mathbf{Y}_m$ is the $R \times N$ matrix which includes the data packets observed at antenna m for all R transmissions;
- $\mathbf{A}_m$ is the $R \times K$ matrix which contains the antenna gains and path coefficients of the mth antenna for all K users (it is assumed that each antenna has a different antenna gain and a different path coefficient for each of the K collided users in every transmission), and the transmitter phase of each packet after every transmission;
- $\mathbf{V}_m$ is the $R \times N$ matrix which represents the white Gaussian noise added to the R observed data packets at antenna m.

Therefore, as depicted in (2.2), $\mathbf{Y}_{L\times N}, \mathbf{A}_{L\times K}$, and $\mathbf{V}_{L\times N}$ are the concatenations of $\mathbf{Y}_m$'s, $\mathbf{A}_m$'s, and $\mathbf{V}_m$'s, respectively, where $m = 1, \ldots, M$. The contents of the matrix $\mathbf{A}_m$ can be shown as

$$\mathbf{A}_m = \begin{bmatrix} a_m(1,1) & \ldots & a_m(1,K) \\ \vdots & \ddots & \vdots \\ a_m(R,1) & \ldots & a_m(R,K) \end{bmatrix} \tag{2.3}$$

and

$$a_m(r,k) = g_m(r,k) f_m(r,k) e^{j\varphi(r,k)} \tag{2.4}$$

with the following definitions.

- $g_m(r,k)$ is the antenna gain of the mth antenna for user k in time slot r, and it is assumed that the antenna gain is constant within that time slot.
- $f_m(r,k)$ is the fading coefficient for the kth user on the transmission path to the mth antenna during time slot r. The fading process is flat and slow enough to assume that $f_m(r,k)$ is constant within the time slot r. $f_m(r,k)$ is complex-valued

and can be expressed by

$$f_m(r,k) = \alpha_m(r,k)e^{j\phi_m(r,k)}. \tag{2.5}$$

It is assumed that the amplitude $\alpha_m(r,k)$ is Rayleigh distributed which is *independent and identically distributed* (i.i.d.) across all users and observations. The phase $\phi_m(r,k)$ is assumed to have a *uniform* distribution over $[-\pi,\pi)$ and they are also i.i.d. across all users and observations.

- $\varphi(r,k)$ is the phase added to the kth packet by the transmitter in time slot r. It is assumed that $\varphi(r,k)$ have a *uniform* distribution over $[-\pi,\pi)$ and they are i.i.d. across all packets and transmissions.

Similarly, the elements of $\mathbf{V}_m$ are denoted as

$$v_m(r,n) = v_m^{real}(r,n) + jv_m^{imag}(r,n) \tag{2.6}$$

where $v_m(r,n)$ is the white Gaussian noise term added to the nth symbol of the packet observed at antenna m in the rth transmission. For all the antennas and the observations, the real and imaginary parts of the additive noise are Gaussian-distributed and mutually independent. In addition, they both have zero mean and variance $\sigma_v^2/2$. Thus, the additive Gaussian noise has zero mean and variance σ_v^2.

2.2. NDMA and BNDMA

2.2.1. NDMA

NDMA is proposed to resolve the collisions in $\lceil K/M \rceil$ slots where K is the collision multiplicity and M is the number of antennas at the base station [18]. Therefore, $K-1$ retransmissions are sufficient to resolve a K-fold collision at the single-antenna case [17]. The signal model that represents the collision problem in (2.1) and (2.2) is also valid for NDMA.

User specific ID sequences, which are mutually orthogonal, are inserted to the beginning of the packets for the collision resolution, and active users are detected by using matched filters at the BS. Each of these matched filters is assigned specifically to one of the user IDs in the system. However, due to the orthogonality requirement, ID sequences grow linearly as the number of users in the system increases. Since the bandwidth, which carries the packet payload, reduces as the ID sequences get longer, size of the population has a negative impact on the throughput performance. As an example, if the packets consist of N bits, the maximum throughput that NDMA can sustain is $N/(N+J)$ when there is a single antenna at the BS [19]. The details of the collision resolution procedure for NDMA can be found in [17, 18].

2.2.2. BNDMA

BNDMA uses blind techniques to detect the collision multiplicity. BNDMA determines the collision multiplicity by using the rank test method, which is described in Section 4.2. The collisions are resolved by employing PARAFAC analysis, which is also known as the trilinear decomposition [18, 19, 20, 21, 22].

In the single-antenna case, tight control of the transmitter phase of each collided packet is required to force the mixing matrix to have a *Vandermonde* structure, whereas the fading process and the antenna gains for each collided user should be constant throughout all transmissions necessary for the collision resolution [19]. These three conditions are required to represent the observed data at the BS as a three-way array to resolve the collision by using PARAFAC analysis. In the presence of spatial diversity, there is no need to control the transmitter phase of the collided packets for PARAFAC, and the fading coefficients can change after every transmission [18]. In this case, observed data are represented as a three-way array by assuming that every antenna has constant gain for each of the collided users throughout all transmissions necessary for the collision resolution [18]. Therefore, BNDMA requires additional restrictions and assumptions over the signaling model represented in (2.1) and (2.2). In Chapter 4, it will be shown that our ICA-based multiple access method works without these restrictions.

The number of transmissions that BNDMA requires for the collision resolution depends on the identifiability condition of PARAFAC method. Identifiability condition, which is actually a corollary of uniqueness of low-rank decomposition of the three-way arrays, is expressed as follows [18, 20].

$$\min(R, K) + \min(N, K) + \min(M, K) \geq 2K + 2. \tag{2.7}$$

Since the packet length is larger than the number of collided users, $N > K$. Therefore, the minimum number of transmissions necessary for the collision resolution is given as [18],

$$R = \begin{cases} 1, & K = 0, 1, \\ 2, & K = 2, 3, \ldots, M \\ K - M + 2, & K = M + 1, M + 2, \ldots \end{cases} \tag{2.8}$$

In the single-antenna case, BNDMA requires $K + 1$ transmissions to resolve a K-fold collision. The maximum throughput for BNDMA is found to be $J/(J + 1)$ for the single-antenna case [19]. Therefore, there is no throughput upper bound for BNDMA as the number of users in the system goes to infinity .

3. INDEPENDENT COMPONENT ANALYSIS

ICA is a statistical method for transforming an observed random vector into components that are statistically as independent from each other as possible. The problem can be represented as follows.

$$\mathbf{y} = \mathbf{A}\mathbf{x} \tag{3.1}$$

where

- $\mathbf{y}$ is the $L \times 1$ observation vector;
- $\mathbf{A}$ is the $L \times K$ unknown mixing matrix;
- $\mathbf{x}$ is the $K \times 1$ unknown vector of the independent components to be found.

It is possible to determine the unknown $\mathbf{x}$ vector and the mixing matrix $\mathbf{A}$ by using ICA, provided that the following conditions hold:

1. The mixed components (elements of the random vector $\mathbf{x}$) should be statistically independent in order to apply the ICA to the source mixing problem [23, 24].
2. The independent data packets should have a *non-Gaussian* distribution.
3. The mixing matrix $\mathbf{A}$ should have full rank and the size condition $L \geq K$ should be met.

The requirements for the independence and the non-Gaussian distribution of the mixed components can be described by the *Central Limit Theorem.* The Central Limit Theorem states that the distribution of the sum of the independent random variables tends toward a Gaussian distribution under certain conditions. Thus, the sum of several independent random variables results in a distribution closer to Gaussian than the distribution of the original random variables which are non-Gaussian. ICA's principle is to obtain the independent components by minimizing the Gaussianity since the distribution of the sum of all independent components is the most Gaussian where one component, as a non-Gaussian random variable, shows the least Gaussian property. Relying on this basic property, ICA finds the unknown mixing matrix $\mathbf{A}$ and the independent component variables in vector $\mathbf{x}$ by only using the observation vector $\mathbf{y}$ in (3.1). To see this better [23], consider a vector $\mathbf{w}$ where $\mathbf{r} = \mathbf{w}^T\mathbf{y}$ and suppose that $\mathbf{z} = \mathbf{A}^T\mathbf{w}$. Then, it can be stated that $\mathbf{r} = \mathbf{w}^T\mathbf{y} = \mathbf{w}^T\mathbf{A}\mathbf{x} = \mathbf{z}^T\mathbf{x}$. Therefore, $\mathbf{r}$ is the linear combination of the independent component variables where the weights are the elements of vector $\mathbf{z}$. Since the sum of even two independent random variables is more Gaussian than the original variables, the linear combination $\mathbf{z}^T\mathbf{x}$ is more Gaussian than any of the independent components and becomes least Gaussian if it equals to only one of the independent components. This is possible if only one of the elements of $\mathbf{z}$ is nonzero. Therefore, the vector $\mathbf{w}$ is considered as a row of the inverse matrix $\mathbf{A}^{-1}$ if it maximizes the non-Gaussianity of $\mathbf{w}^T\mathbf{y}$ since it results in a $\mathbf{z}$ which has only one nonzero component. As a result, ICA obtains the inverse of matrix $\mathbf{A}$ by maximizing the non-Gaussianity and the vector $\mathbf{x}$ can be estimated as $\mathbf{x} = \mathbf{A}^{-1}\mathbf{y}$. In ICA estimation, several measures of non-Gaussianity such as *kurtosis, negentropy, minimization of mutual information, or maximum likelihood estimation* can be used [23]. There are several fast ICA algorithms which depend on these measures [25, 26].

Before applying ICA, it is useful to preprocess the observed data through centering and whitening [23]. The source mixing problem becomes simpler and better conditioned for ICA after the preprocessing.

Centering is used to make $\mathbf{y}$ in equation (3.1) a zero-mean vector. This is simply accomplished by subtracting the mean vector $E\{\mathbf{y}\}$ from $\mathbf{y}$:

$$\mathbf{y} - E\{\mathbf{y}\} = \mathbf{A}\mathbf{x} - \mathbf{A}E\{\mathbf{x}\} = \mathbf{A}(\mathbf{x} - E\{\mathbf{x}\}) \tag{3.2}$$

As shown in (3.2), we also make $\mathbf{x}$ a zero-mean vector by using centering. After employing the ICA, we can complete the estimation of $\mathbf{x}$ by adding the mean vector of $\mathbf{x}$ back to the centered estimates. The mean vector of $\mathbf{x}$ is given by $\mathbf{A}^{-1}E\{\mathbf{y}\}$ since

$$\mathbf{A}^{-1}E\{\mathbf{y}\} = \mathbf{A}^{-1}\mathbf{A}E\{\mathbf{x}\} = E\{\mathbf{x}\}. \tag{3.3}$$

The whitening procedure applies a linear transformation on $\mathbf{y}$ to obtain $\mathbf{y}_{new} = \mathbf{B}\mathbf{y} = \mathbf{B}\mathbf{A}\mathbf{x}$, where

$$E\{\mathbf{y}_{new}\mathbf{y}_{new}^T\} = \mathbf{I}. \tag{3.4}$$

Thus, the ICA problem is still the same (the problem is to find the unknown independent components of vector $\mathbf{x}$) with a new unknown mixing matrix

$$\mathbf{A}_{new} = \mathbf{B}\mathbf{A}. \tag{3.5}$$

After whitening is applied, the new mixing matrix $\mathbf{A}_{new}$ is orthogonal. This can be shown as follows (if the independent components in $\mathbf{x}$ have zero mean and unit variance)

$$E\{\mathbf{y}_{new}\mathbf{y}_{new}^T\} = \mathbf{A}_{new}E\{\mathbf{x}\mathbf{x}^T\}\mathbf{A}_{new}^T = \mathbf{A}_{new}\mathbf{A}_{new}^T = \mathbf{I}. \tag{3.6}$$

Whitening reduces the number of parameters to be estimated since the new orthogonal mixing matrix $\mathbf{A}_{new}$ has fewer degrees of freedom compared to $\mathbf{A}$. There are several ways of finding the transformation matrix $\mathbf{B}$ such as *eigenvalue decomposition* (EVD) or *singular value decomposition* (SVD).

So far, the definition of the source mixing problem in equation (3.1) has not contained any additive noise term, which is not the case in many applications. In wireless systems, the transmission channel also suffers from the additive noise which is generally modelled to be Gaussian-distributed. Hence, the ICA-based collision resolution protocol should work properly in the presence of Gaussian noise. In the next section, the information is given about the ICA method in the presence of Gaussian noise [27].

3.1. ICA in the Presence of Gaussian Noise

The additive Gaussian noise may be present in the source mixing process. In this case, the problem represented by equation (3.1) becomes

$$\mathbf{y} = \mathbf{A}\mathbf{x} + \mathbf{v}. \tag{3.7}$$

In the noiseless case, it is sufficient to find the inverse of the mixing matrix $\mathbf{A}$ to estimate the independent components in $\mathbf{x}$. However, the nonlinear reconstruction of $\mathbf{x}$ is necessary because of the additive term $\mathbf{v}$ in the noisy ICA model.

Maximum likelihood estimation is one of the popular ICA methods as mentioned previously. This method is used to solve the noisy ICA problem, as well as the noiseless one described in [23]. First, the likelihood of the noisy ICA model is formulated. For this purpose, the negative log-likelihoods (log-densities) of the elements in vector $\mathbf{x}$ are used. If $\mathbf{x} = [x_1\ x_2\ \dots\ x_K]^T$ and the density for each element x_i is $p_{x_i}(x_i)$, the negative log-likelihood for x_i is $f_{x_i}(x_i)$ = - $\log p_{x_i}(x_i)$. The noise $\mathbf{v}$ in equation (3.7) is Gaussian with covariance matrix $\mathbf{\Sigma}$. If the densities of x_i and the noise covariance matrix $\mathbf{\Sigma}$ are known, the log-likelihood for the noisy model is formulated as below [27]. Here, it is assumed that T observation vectors, $\mathbf{y}(t), t = 1, \dots, T$, are collected for the model and all x_i have identical densities (hence the same log density denoted as $f(x_i)$) [27].

$$\log L(\mathbf{A}, \mathbf{x}(1), \dots, \mathbf{x}(T)) = -\sum_{t=1}^{T} \left[\frac{1}{2} \|\mathbf{A}\mathbf{x}(t) - \mathbf{y}(t)\|^2_{\mathbf{\Sigma}^{-1}} + \sum_{i=1}^{K} f(x_i(t)) \right] + C \tag{3.8}$$

where $\|\mathbf{e}\|^2_{\mathbf{\Sigma}^{-1}}$ is defined as $\mathbf{e}^T\mathbf{\Sigma}^{-1}\mathbf{e}$ and C is an irrelevant constant. The maximization of this likelihood is necessary for the joint estimation of $\mathbf{A}$ and $\mathbf{x}(t), t = 1, \dots, T$. However, this is not an easy task because both $\mathbf{A}$ and $\mathbf{x}(t)$ are unknown. There are $K \times L + K \times T$ variables to be determined, since $\mathbf{A}$ is an $L \times K$ matrix and $\mathbf{x}(t)$ is a $K \times 1$ vector, and some approximations are needed to reduce the dimensions of the problem. After taking the gradient of the Lagrangian of the log-likelihood in equation (3.8) with respect to $\mathbf{x}(t)$ and equating the result to 0, the following is obtained (denoting by $\hat{\mathbf{A}}$

and $\hat{\mathbf{x}}(t)$ are the estimates for $\mathbf{A}$ and $\mathbf{x}(t)$, respectively) [27].

$$\hat{\mathbf{A}}^T\boldsymbol{\Sigma}^{-1}\hat{\mathbf{A}}\hat{\mathbf{x}}(t) - \hat{\mathbf{A}}^T\boldsymbol{\Sigma}^{-1}\mathbf{y}(t) + f'(\hat{\mathbf{x}}(t)) - \hat{\mathbf{x}}(t) = 0, \tag{3.9}$$

which gives

$$\hat{\mathbf{A}}^T\boldsymbol{\Sigma}^{-1}\hat{\mathbf{A}}\hat{\mathbf{x}}(t) = \hat{\mathbf{A}}^T\boldsymbol{\Sigma}^{-1}\mathbf{y}(t) - f'(\hat{\mathbf{x}}(t)) + \hat{\mathbf{x}}(t). \tag{3.10}$$

For simplicity, assume that $\mathbf{A}$ is a square matrix. By multiplying both sides of equation (3.10) by $\hat{\mathbf{A}}^{-1}\boldsymbol{\Sigma}\hat{\mathbf{A}}^{-T}$, one obtains

$$\hat{\mathbf{x}}(t) = \hat{\mathbf{A}}^{-1}\mathbf{y}(t) - \hat{\mathbf{A}}^{-1}\boldsymbol{\Sigma}\hat{\mathbf{A}}^{-T}(f'(\hat{\mathbf{x}}(t)) - \hat{\mathbf{x}}(t)). \tag{3.11}$$

Two assumptions are made in [27] and two different approximations is obtained from equation (3.11). First, it is assumed that the noise amplitude is small and f' is a smooth function. Then, $\hat{\mathbf{x}}(t)$ is replaced with $\hat{\mathbf{A}}^{-1}\mathbf{y}(t)$ and the following approximation is obtained [27].

$$\hat{\mathbf{x}}(t) = \hat{\mathbf{A}}^{-1}\mathbf{y}(t) - \hat{\mathbf{A}}^{-1}\boldsymbol{\Sigma}\hat{\mathbf{A}}^{-T}(f'(\hat{\mathbf{A}}^{-1}\mathbf{y}(t)) - \hat{\mathbf{A}}^{-1}\mathbf{y}(t)) \tag{3.12}$$

The second approximation can be obtained by assuming that $\boldsymbol{\Sigma} = \sigma^2\mathbf{A}\mathbf{A}^T$. In this assumption, the noise is added to the independent components before mixing them. In such a case , the noisy mixing problem in equation (3.7) is represented as $\mathbf{y} = \mathbf{A}\mathbf{x} + \mathbf{v} = \mathbf{A}\mathbf{x} + \mathbf{A}\mathbf{n}$, and it is possible to represent the noise covariance matrix as $\boldsymbol{\Sigma} = E\{\mathbf{A}\mathbf{n}\mathbf{n}^T\mathbf{A}^T\} = \mathbf{A}E\{\mathbf{n}\mathbf{n}^T\}\mathbf{A}^T = \mathbf{A}\sigma^2\mathbf{I}\mathbf{A}^T = \sigma^2\mathbf{A}\mathbf{A}^T$ (the noise terms in vector $\mathbf{n}$ added to each independent component are independent, uncorrelated and have a unique variance of σ^2). As a result, the second approximation is obtained by replacing $\boldsymbol{\Sigma}$ in equation (3.11) with $\sigma^2\hat{\mathbf{A}}\hat{\mathbf{A}}^T$ [27]:

$$\hat{\mathbf{x}}(t) = h(\hat{\mathbf{A}}^{-1}\mathbf{y}(t)). \tag{3.13}$$

The dimensions of the problem is reduced to the dimensions of the mixing matrix $\mathbf{A}$ by using either (3.12) or (3.13) for the optimization of (3.8). Equation (3.12) can be used if f' is smooth and the noise covariance matrix is far from the form $\sigma^2\mathbf{A}\mathbf{A}^T$ [27]. Otherwise, it is better to use (3.13). Depending on the distribution of x_i, special h functions are given in [27]. For example, x_i may have *uniform distribution* of unit variance. In this case, f' is not smooth, and it is better to use approximation (3.13). The uniform distribution is a sub-Gaussian distribution since the sub-Gaussian distributions are flatter and have lighter tails with respect to Gaussian distributions. Then, the function h is obtained as a *truncation operator* which is $h(u)$ =sign$(u)\min(|\ u\ |, \sqrt{3})$. This is also intuitively correct because the uniformly distributed random variables of unit variance cannot have values outside the interval $[-\sqrt{3}, \sqrt{3}]$. As a second example, x_i may have *binary distribution* which is extremely sub-Gaussian. If x_i have unit variance, the truncation operator is $h(u)$ =sign(u), since the value for x_i is either +1 or -1.

The *alternating variables* method achieves the optimization of the likelihood (3.8) by using the approximations introduced in this section. According to this approach, an objective function is first optimized with respect to $\mathbf{A}$ for fixed $\mathbf{x}(t)$, and then optimized with respect to $\mathbf{x}(t)$ for fixed $\mathbf{A}$ iteratively. The steps are as follows:

1. Take an initial mixing matrix value $\hat{\mathbf{A}}_0$. Let $j = 1$.
2. Compute $\hat{\mathbf{x}}_j(t)$ by using either (3.12) or (3.13) where $\hat{\mathbf{A}}_{j-1}$ is the estimate of $\mathbf{A}$. Normalize the components of $\hat{\mathbf{x}}_j(t)$ to have unit variance.
3. Update $\hat{A}_j = E\{\mathbf{y}(t)\hat{\mathbf{x}}_j^T(t)\}[E\{\hat{\mathbf{x}}_j(t)\hat{\mathbf{x}}_j^T(t)\}]^{-1}$
4. Increment j and go back to step 2 if not converged.

The preprocessing of the observed data such as sphering (or whitening) is also useful for the performance of the above method. By doing that, the covariance matrix of $\mathbf{y}(t)$ is made equal to unity so that $E\{\mathbf{y}(t)\mathbf{y}^T(t)\} = \mathbf{I}$. After doing this, there is no need for the matrix inversion of $\hat{\mathbf{A}}$ to be used in approximation (3.12) or (3.13). Since the additive noise and independent components are uncorrelated (and assume that the independent components have unit variance), after sphering (or whitening) the data

$E\{\mathbf{y}(t)\mathbf{y}^T(t)\} = \mathbf{A}E\{\mathbf{x}(t)\mathbf{x}^T(t)\}\mathbf{A}^T + \mathbf{\Sigma} = \mathbf{A}\mathbf{A}^T + \mathbf{\Sigma} = \mathbf{I}$. Thus, $\hat{\mathbf{A}}^{-1}$ can be replaced by $\hat{\mathbf{A}}^T(\mathbf{I} - \mathbf{\Sigma})^{-1}$. In addition to this simplification, the stability of the method can be improved by orthogonalizing the mixing matrix estimate $\hat{\mathbf{A}}$ after every iteration so that $\hat{\mathbf{A}}\hat{\mathbf{A}}^T = \mathbf{I} - \mathbf{\Sigma}$.

4. ICA-BASED MULTIPLE ACCESS METHOD

4.1. Retransmission Protocol and the ICA-Based Collision Resolution

The signaling model in (2.1) depends on the BS-controlled retransmissions of collided packets. The retransmission protocol has the following properties.

- The BS checks each transmission slot online to detect any packet collisions by using a multiplicity detection criterion which will be described in Section 4.2. If the BS detects a collision at any time slot, it sets on a retransmission flag which stops the new packet transmissions.
- If the retransmission flag is on, the users who were active at the previous slot retransmit the same packets until the retransmission flag is off. Those who were inactive during the previous slot, block any possible transmissions until the retransmission flag is off.
- The retransmissions continue till the BS determines the collision multiplicity, at which point the retransmission flag is set off and ICA is employed for the collision resolution in the same slot.

Details of the collision multiplicity detection are described in the next chapter.

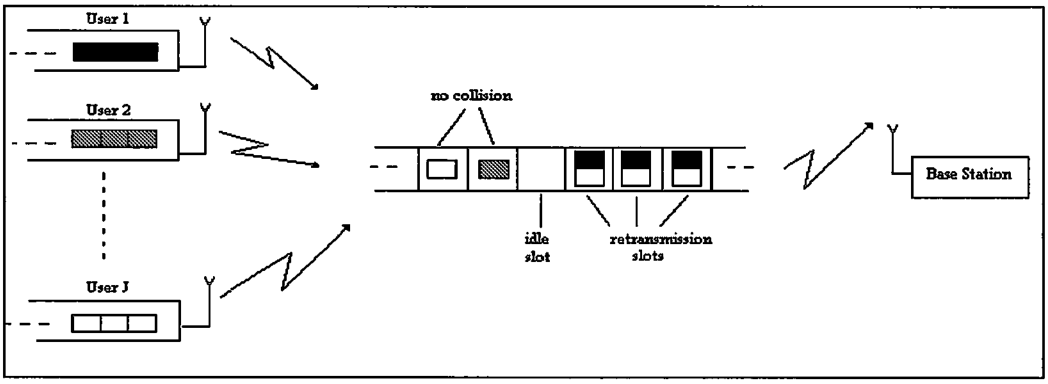

Figure 4.1. Packet transmissions in slotted wireless system

During retransmissions, users in the wireless system may generate new packets to transmit. Every user should have a buffer to store these packets, which are to be transmitted when the channel is available. In this thesis, each user is assumed to have an infinite-length packet buffer as shown in Figure 4.1.

After the collision multiplicity is determined, ICA is employed for the collision resolution. The steps of the ICA algorithm to be used are given in Section 3.1. If the distribution of the bits in the independent packets is assumed to be close to the binary distribution, equation (3.13) will be chosen for the ICA algorithm instead of equation (3.12). Because, in that case, the log-densities for the binary-distributed packets will not be smooth and equation (3.13) needs to be used as mentioned in Section 3.1 and [27]. In this chapter, the subscripts of matrices $\mathbf{Y}_{L\times N}, \mathbf{A}_{L\times K}$, $\mathbf{S}_{K\times N}$, and $\mathbf{V}_{L\times N}$ will be dropped for simplicity.

Before applying the ICA algorithm, observed data is whitened by using *sphering* [33]. After the observed data are sphered, the new $K\times K$ data matrix is $\mathbf{X} = \triangle^{-\frac{1}{2}}\mathbf{U}^H\mathbf{Y}$ where the $K \times K$ diagonal matrix $\triangle$ and the $L \times K$ matrix $\mathbf{U}$ corresponds to the K principle eigenvalues and eigenvectors of $L \times L$ correlation matrix estimate $\mathbf{Y}\mathbf{Y}^H/N$, respectively. Let's consider that

$$\mathbf{M} = \triangle^{-\frac{1}{2}}\mathbf{U}^H. \tag{4.1}$$

Then, the collision problem in (2.1) after sphering is

$$\mathbf{X} = \mathbf{MY} = \mathbf{MAS} + \mathbf{MV} = \mathbf{BS} + \mathbf{MV}. \tag{4.2}$$

Before sphering, the observed data is also centered to have independent data packets with zero mean.

The dimension of the new mixing matrix $\mathbf{B}$ is $K \times K$ and $\mathbf{X}\mathbf{X}^H/N = \mathbf{I}$. Since the additive noise denoted by $\mathbf{V}$ is Gaussian-distributed, the new $K \times N$ noise matrix $\mathbf{MV}$ also has Gaussian distribution. If $\hat{\mathbf{B}}$ and $\hat{\mathbf{S}}$ are the estimates of $\mathbf{B}$ and $\mathbf{S}$, respectively, the ICA algorithm described in Section 3.1 has the following steps for the collision resolution (expectations in the steps in Section 3.1 are replaced by averages over N samples):

1. Take an initial mixing matrix value $\hat{\mathbf{B}}_0$. Let $j = 1$.
2. Compute $\hat{\mathbf{S}}_j$ by using a truncation operator where $\hat{\mathbf{S}}_j$ =sgn(Re$\{\hat{\mathbf{B}}_{j-1}^{-1}\mathbf{X}\}$) because it is assumed that the independent packets are binary distributed.
3. Update $\hat{\mathbf{B}}_j = [\mathbf{X}\hat{\mathbf{S}}_j^T/N][\hat{\mathbf{S}}_j\hat{\mathbf{S}}_j^T/N]^{-1}$.
4. Increment j and go back to step 2 if not converged.

By assuming that the independent packets have unit variance and are independent of the additive Gaussian noise, and the observed data is sphered, the following relations can be obtained.

$$\mathbf{X}\mathbf{X}^H/N = \mathbf{I} = \mathbf{B}\underbrace{[\mathbf{S}\mathbf{S}^H/N]}_{\approx\mathbf{I}}\mathbf{B}^H+\mathbf{B}\underbrace{[\mathbf{S}\mathbf{V}^H/N]}_{\approx\mathbf{0}}\mathbf{M}^H+\mathbf{M}\underbrace{[\mathbf{V}\mathbf{S}^H/N]}_{\approx\mathbf{0}}\mathbf{B}^H+\mathbf{M}\underbrace{[\mathbf{V}\mathbf{V}^H/N]}_{\approx\sigma_v^2\mathbf{I}}\mathbf{M}^H, \tag{4.3}$$

and

$$\mathbf{I} \approx \mathbf{B}\mathbf{B}^H + \sigma_v^2\mathbf{M}\mathbf{M}^H. \tag{4.4}$$

After obtaining (4.4), the stability of the algorithm can be improved by orthogonalizing the matrix $\hat{\mathbf{B}}$ so that $\hat{\mathbf{B}}\hat{\mathbf{B}}^H = \mathbf{I} - \sigma_v^2\mathbf{M}\mathbf{M}^H$ after every iteration [27].

4.2. Blind Collision Detection

The detection of collision multiplicity, K, is necessary for the BS to determine the number of retransmissions and to find the number of independent packets to be resolved by ICA. The information available at the BS is the mixture of original data packets. Therefore, the BS has to determine K blindly.

If the noise in equation (2.1) is not present, collisions can be detected by simply checking the rank of the observed data matrix $\mathbf{Y}_{L\times N}$. Since the number of users K is much less than the packet length N, the matrix $\mathbf{S}_{K\times N}$ is full-rank and $\text{rank}(\mathbf{S}_{K\times N}) = K$. If the mixing matrix $\mathbf{A}_{L\times K}$ is full-rank (which is guaranteed under the i.i.d assumption for $a_m(r,k)$), $\text{rank}(\mathbf{A}_{L\times K}) = \min(L,K)$. Therefore, the matrix $\mathbf{Y}_{L\times N}$ is full-rank when the number of collided users is greater than or equal to the number of observations because $\text{rank}(\mathbf{Y}_{L\times N}) = L$ if $K \geq L$. However, $\text{rank}(\mathbf{Y}_{L\times N}) = K$ if $K < L$, so $\mathbf{Y}_{L\times N}$ loses rank.

By using the above property, the BS can check the rank of the observed data matrix after every retransmission until the matrix $\mathbf{Y}_{L\times N}$ loses rank, and at that point the corresponding rank gives the collision multiplicity, K. Therefore, if K is an integer multiple of the number of antennas at the BS, M,

$$R = \lceil K/M \rceil + 1, \tag{4.5}$$

and otherwise

$$R = \lceil K/M \rceil. \tag{4.6}$$

As an example, the number of transmissions to detect a K-fold collision is $K+1$ when there is a single antenna at the BS.

If the collision problem in equation (2.1) is considered, the above approach will no longer be true since noise is present. In this case, there are several blind methods to detect the number of collided users K such as the *rank test* [19] and the *information-theoretic criteria method* [34, 35]. Both determine the collision multiplicity blindly by using the eigenvalues of the correlation matrix $\mathbf{Y}_{L\times N}\mathbf{Y}^H_{L\times N}/N$.

In the rank test method, the eigenvalues of the correlation matrix $\mathbf{Y}_{L\times N}\mathbf{Y}^H_{L\times N}/N$ are estimated after every transmission and sorted in decreasing order as $\lambda_1 \geq \lambda_2 \geq \ldots \geq \lambda_l \geq \ldots \geq \lambda_L$. Then the eigenvalues are checked against a tolerance threshold T

[19], and if

$$\lambda_l < T, \qquad l = 1, \ldots, L \tag{4.7}$$

for any of the eigenvalues, the correlation matrix is decided to be rank-deficient and the collision multiplicity is detected as $K = l - 1$. Otherwise, the collided packets are retransmitted and the same checks are done again. The threshold value T can be determined depending on the noise power. The remaining $L - l + 1$ eigenvalues, which are smaller than T, belong to additive Gaussian noise when the collision multiplicity is detected. In the noiseless case, when the signal-to-noise ratio (SNR) is infinity, these eigenvalues are zero.

The information-theoretic criterion used for the collision detection in this thesis is the *Akaike information criterion* (AIC) [34, 35]. After every transmission, AIC is estimated by putting the eigenvalues $\lambda_1 \geq \lambda_2 \geq \ldots \geq \lambda_L$ of the correlation matrix in [34, 35]

$$\mathrm{AIC(l)} = -2(\mathrm{L}-\mathrm{l})\mathrm{N}\ln\frac{\mathrm{G}(\lambda_{\mathrm{l}+1},\ldots,\lambda_{\mathrm{L}})}{\mathrm{A}(\lambda_{\mathrm{l}+1},\ldots,\lambda_{\mathrm{L}})} + 2\mathrm{l}(2\mathrm{L}-\mathrm{l}) \tag{4.8}$$

where $l = 0, \ldots, L-1$, and A and G denote the arithmetic and the geometric means of their arguments, respectively. Then, the following condition is checked for $l = 0, \ldots, L-2$,

$$\mathrm{AIC(l)} < \mathrm{AIC(l+1)}, \tag{4.9}$$

and if it is satisfied, the collision multiplicity is decided to be $K = l$. Otherwise, the collided packets are retransmitted and the above steps are repeated.

Both blind methods above may underestimate or overestimate the collision multiplicity, affecting the ICA performance in terms of throughput or the transmission delay. In case of underestimation, the ICA method tries to resolve the underestimated number of packets and generally results in bit errors. Because ICA attempts to separate fewer packets than the actual quantity, some of the packets are never estimated and their loss causes a deterioration in throughput performance. In case of overestimation, some channel slots are wasted by unnecessary retransmissions and therefore the delay performance suffers.

When compared to AIC, the rank test method has the flexibility of deciding on the value of the tolerance threshold T by checking the overestimation/underestimation possibilities. However, it is sometimes hard to select an appropriate threshold for the system, especially in fast fading channels which makes AIC more preferable.

4.3. Performance of the ICA-Based Collision Resolution with Blind Collision Detection

When collisions are detected blindly and resolved by employing ICA, performance improvements in terms of mean transmission delay and the system throughput are expected over simple random access protocols such as slotted-ALOHA. This is because the BS controls the number of retransmissions (which can be reduced by using spatial diversity), and one channel slot can carry more than one packet (which can be resolved even within that channel slot depending on the size of the spatial diversity). Therefore, less number of channel slots are wasted and more packets are resolved per channel slot.

There are four important factors that affect the throughput and delay performance of ICA-based collision resolution with blind collision detection. These are the *performance of the collision detector*, *bit errors*, *spatial diversity*, and the *traffic load of the system.*

The performance of the blind collision detector is important for reasons explained in Section 4.2. If the collision detector underestimates the collision multiplicity K, the size condition $L \geq K$ is not satisfied because of insufficient retransmissions. Thus, ICA attempts to resolve fewer number of packets than the actual quantity, which results in a deterioration in throughput performance. In case of overestimation, more channel slots than necessary are wasted to detect the collision multiplicity, and therefore, the delay performance suffers.

Throughput performance suffers also because of bit errors. Even if the collision multiplicity is determined correctly, ICA may result with bit errors while separating the data packets. Error correction coding can be used to overcome this situation. However, there may be still residual bit errors which are beyond the correction capability of the code. In such a case, these packets are considered as corrupted and they are lost. Therefore, the throughput of the system decreases.

If the antenna diversity applied at the BS, number of observations at each transmission is equal to the number of antennas at the base station. Therefore, fewer retransmissions are required to determine the collision multiplicity, and the delay performance improves. In such a case, throughput performance also improves since it is possible to resolve more than one packet per slot.

Traffic load, or the *packet arrival rate of the system*, has a significant impact on the throughput and delay performance. More users transmit in higher traffic loads, and more packets collide. Thus, higher number of retransmissions is required to detect and resolve the collision, and the transmission delay increases. We should also expect higher throughput since the packet arrival rate of the system increases.

In the following section, a quantitative model is given depending on the analytical information in [17, 18] to obtain theoretical bounds for the throughput and mean delay performance when the SNR is infinity. Then, the experimental results in Chapter 5 are compared with these optimum results.

4.4. Quantitative Model for the Collision Resolution with Blind Collision Detection

In this section, the purpose is to find a mathematical representation for the performance of the system throughput and the mean transmission delay depending on the varying traffic load by using the analytical approach given in [17, 18, 19]. In order to achieve this, the *mathematical expression for the consecutive number of channel slots used for the collision resolution* (also called *epochs*) and the *queue model for the packet buffer of the mobile users* are defined. It is assumed that the packets are resolved without any bit errors and the SNR equals infinity so that the collision multiplicity can be determined by simply checking the rank of the observed data matrix.

4.4.1. Epoch Definitions

Epoch is the mathematical representation of the consecutive number of channel slots used for the collision resolution. If we consider the analytical framework in [17, 18], the length of an epoch is a random variable which depends on the number of collided users at the beginning of that epoch. If there are M antennas and K collided users, $\{K/M\}$ gives the epoch length to detect and resolve the collision where the epoch length operator $\{\ \}$ acts as an integer ceiling operator when K is not an integer multiple of M. Otherwise, $\{K/M\} = K/M + 1$.

As an example, let us consider the case where there is a single antenna at the BS. If K users collide, the epoch length will be $K + 1$ as shown in Figure 4.2.

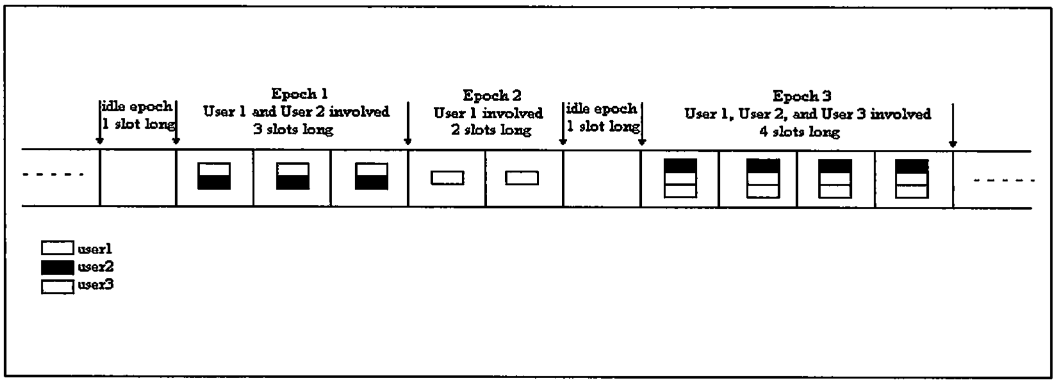

Figure 4.2. Epoch flow in the transmission channel

The following epoch distributions for the ICA-based method are modified from the distributions for NDMA in [18].If the total number of users in the system is denoted by J, the distribution for the *normal* epoch length is as follows.

- If $\{J/M\} \neq J/M + 1$, the epoch length (denoted by H) in which the collision is detected and resolved has the following distribution.

$$\begin{aligned} P[H = h] &= \sum_{r=1}^{U} b_J[M(h-1) - 1 + r + \delta(h-1)] + b_J[0]\delta(h-1), \\ &\quad h = 1, \ldots, \{J/M\} \end{aligned} \tag{4.10}$$

where $U = \min[(M - \delta(h-1)), (J - (h-1)M + \delta(\{J/M\} - h))]$, $b_J[j] = \binom{J}{j}(1-P_e)^j(P_e)^{J-j}$ is the binomial mass function, and P_e is the probability that a user is not active at the beginning of an epoch.

- If $\{J/M\} = J/M + 1$, the distribution is

$$\begin{aligned} P[H = h] &= \sum_{r=1-\delta(J/M+1-h)}^{U} b_J[M(h-1) - 1 + r + \delta(h-1) + \delta(J/M + 1 - h)] \\ &\quad + b_J[0]\delta(h-1), \quad h = 1, \ldots, \{J/M\} \end{aligned} \tag{4.11}$$

where $U = \min[(M - \delta(h-1)), (J - (h-1)M)]$.

There are two types of epochs for a specific user which are classified as *relevant epochs* where the corresponding user transmits and *irrelevant epochs* where the corresponding user does not transmit [17]. As an example, *Epoch 1* and *Epoch 3* in Figure 3.2 are relevant epochs to *user2*. *Epoch 2* and all *idle epochs* are irrelevant epochs to *user2*.

Distribution of the *relevant epoch* is expressed as follows.

$$P[H_r = h] = \sum_{r=1}^{U} b_{J-1}[M(h-1) + \delta(h-1) - 2 + r], \quad h = 1, \cdots, \{J/M\} \tag{4.12}$$

where $U = \min[(M - \delta(h-1)), (J - (h-1)M + \delta(\{J/M\} - h))]$.

Distribution of the *irrelevant epoch* is expressed as follows.

- If $\{(J-1)/M\} \neq (J-1)/M+1$, the distribution is

$$\begin{aligned} P[H_{ir}=h] &= \sum_{r=1}^{U} b_{J-1}[M(h-1)-1+r+\delta(h-1)] + b_{J-1}[0]\delta(h-1), \\ & h = 1,\cdots,\{(J-1)/M\} \end{aligned} \tag{4.13}$$

where $U = \min\left[(M-\delta(h-1)), (J-1-(h-1)M+\delta(\{(J-1)/M\}-h))\right]$

- If $\{(J-1)/M\} = (J-1)/M+1$, the distribution is

$$\begin{aligned} P[H_{ir}=h] &= \sum_{r=1-\delta((J-1)/M+1-h)}^{U} b_{J-1}[M(h-1)-1+r+\delta(h-1) \\ & +\delta((J-1)/M+1-h)] + b_{J-1}[0]\delta(h-1), \\ & h = 1,\cdots,\{(J-1)/M\} \end{aligned} \tag{4.14}$$

where $U = \min\left[(M-\delta(h-1)), (J-1-(h-1)M)\right]$.

4.4.2. Queue Model for the User's Buffer

Each user's packet buffer is assumed to be a queue with infinite length, where the packets in the queue are waiting to be processed by the transmission channel. The number of packets arriving at each user's buffer is generated by a *Poisson* process which is independent for every user and has a per-user arrival rate of λ packets/slot.

In order to derive a mathematical expression for P_e, previous works in [17, 18] focus on q_l which denotes the number of packets in a user's buffer at the beginning of each epoch, and consider q_l as the state variable of a Markov chain. As a result, the following state transition is obtained.

$$q_{l+1} = \begin{cases} q_l - 1 + r_l, & q_l > 0, \\ r_l, & q_l = 0 \end{cases} \tag{4.15}$$

where r_l denotes the number of new packets that arrives to the user's buffer.

After the *steady state* analysis of the Markov chain with state transitions in (4.15), the following relationship is obtained to calculate P_e based on the detailed analytical procedure in [17].

$$P_e = 1 - \lambda E[H]. \tag{4.16}$$

Since the first moment of H depends on P_e, equation (4.16) can be used to numerically solve for P_e when λ is given. After P_e is calculated, it is possible to analytically express the throughput and delay as shown next.

4.4.3. Mathematical Representation for Throughput and Delay

The system throughput and transmission delay for a given λ are calculated by using normal, relevant, and irrelevant epoch moments whose distributions are given in Section 4.4.1. It is also known that the probability P_e, which the epoch distributions depend on, can be obtained by using equation (4.16).

System throughput is expressed as the ratio of the average number of collided users at the beginning of an epoch and the average length of the epoch [18].

$$\lambda_T = \frac{J(1-P_e)}{E[H]}. \tag{4.17}$$

If it is assumed that each user's packet buffer is modelled as an M/G/1 queue with server vacation, the relevant and irrelevant epochs can be considered as the service time and the vacation time, respectively [17]. Then, the mean transmission delay D for a user's packet through M/G/1 queue with server vacation is expressed approximately as follows [36, 3].

$$D = E[H_r] + \frac{\lambda E[H_r^2]}{2(1-\lambda E[H_r])} + \frac{E[H_{ir}^2]}{2E[H_{ir}]}. \tag{4.18}$$

4.4.4. Results for Throughput and Delay Performance in the Single-Antenna Case

As an example, the results for the throughput and delay performance of the system are obtained when there is no spatial diversity at the BS. Single-antenna case is chosen on purpose since it is easier to follow the mathematical procedure to calculate the throughput and delay.

Epoch definitions are simpler for the single-antenna case. The distributions for normal, relevant, and irrelevant epochs are given in equations (4.19), (4.20), and (4.21), respectively [19].

$$\begin{aligned} P[H=h] &= \binom{J}{h-1}(1-P_e)^{h-1}P_e^{J-h+1}, \\ & \quad h = 1,\ldots,J+1, && (4.19) \\ P[H_r=h] &= \binom{J-1}{h-2}(1-P_e)^{h-2}P_e^{J-h+1}, \\ & \quad h = 2,\ldots,J+1, && (4.20) \\ P[H_{ir}=h] &= \binom{J-1}{h-1}(1-P_e)^{h-1}P_e^{J-h}, \\ & \quad h = 1,\ldots,J. && (4.21) \end{aligned}$$

We need to solve for the probability P_e to obtain analytical results for throughput and mean delay. For this purpose, $E[H]$ is expressed as follows.

$$\begin{aligned} E[H] &= \sum_{h=1}^{J+1} hP[H=h] \\ &= \sum_{h=1}^{J+1} h\binom{J}{h-1}(1-P_e)^{h-1}P_e^{J-h+1}. && (4.22) \end{aligned}$$

By using change of variables $m = h-1$,

$$\begin{aligned} E[H] &= \sum_{m=0}^{J}(m+1)\binom{J}{m}(1-P_e)^{m}P_e^{J-m} \\ &= E[m+1] && (4.23) \end{aligned}$$

where m is binomial-distributed as shown above. Due to the properties of the binomial distribution [37],

$$E[H] = J(1 - P_e) + 1. \tag{4.24}$$

If the above expression is inserted into equation (4.16), the probability P_e is solved as

$$P_e = 1 - \frac{\lambda}{1 - \lambda J}. \tag{4.25}$$

The maximum sustainable packet arrival rate per user, λ_{max}, is obtained when the probability that a user has an empty buffer is zero [19]. By setting $P_e = 0$ in (4.25) and solving for the packet arrival rate, it is found that $\lambda_{max} = 1/(J+1)$ packets/slot. Therefore, the maximum throughput for the single-antenna case is $J/(J+1)$, which converges to 1 as the number of users in the system increase.

After P_e is obtained as in (4.25), the mean delay can also be determined by simply using equation (4.18) since the moments of relevant and the irrelevant epochs depend on P_e. The following figure shows the mean delay performance for the single-antenna case obtained by using equation (4.18).

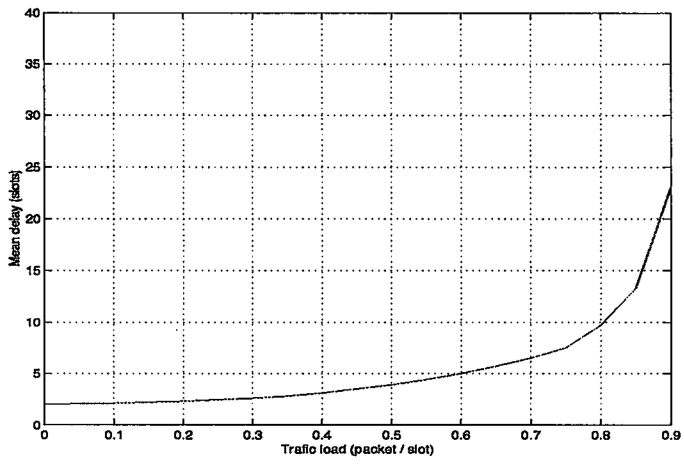

Figure 4.3. Mean delay (D) versus traffic load (λJ) depending on the mathematical results

5. SIMULATIONS AND DISCUSSIONS

Simulations to test the throughput and delay performance of the ICA-based collision resolution with blind collision detection are based on the following:

- Each user has a packet buffer of infinite length which is fed by a Poisson process with an arrival rate of λ packets/slot. Therefore, the traffic load or the total packet arrival rate of the system equals to λJ [37].
- AIC is used to determine the collision multiplicity blindly.
- In order to detect the bit errors after resolution, the packets are encoded with 16-bit CRC code [38, 33]. In addition, the Hamming code is used for error correction. The packets with residual bit errors are regarded as corrupted.
- The packet length, without CRC encoding and error correction code, is decided to be 274 bits long [19, 18].
- Number of users in the system is $J = 16$.
- The transmission channel has flat fading process with Rayleigh distributed amplitude and uniform-distributed phase over $[-\pi, \pi)$. The fading process is slow enough to be constant during one channel slot. The channel noise is modelled as additive white Gaussian.
- The transmitter phase is random and has uniform distribution over $[-\pi, \pi)$. The receiver phase is assumed to be zero.
- Throughput is estimated as the ratio of average number of packets resolved with no bit errors at the end of an epoch and the average epoch length.
- Average transmission delay is the waiting time in the buffer and the transmission time in the channel.
- Average SNR is not taken into account, and SNR is defined as the signal power of one packet over the noise power.
- Sufficient number of channel slots are simulated is sufficient to ensure convergence.

In this chapter, experimental results for delay and throughput performance of the ICA-based multiple access protocol are given first. Then, the delay distribution is shown for various SNR and traffic load scenarios. Next, experimental results for delay and throughput performance of NDMA and BNDMA methods are compared to those of the ICA-based method.

5.1. Simulation Results for ICA-Based Multiple Access Method

5.1.1. Throughput and Delay Performance for the Single-Antenna Case

First, the throughput and delay performance is tested under the infinite-SNR scenario, where the collision multiplicity is determined by simply checking the rank of the observation matrix after each retransmission. Figure 5.1 which illustrates the delay performance of ICA is consistent with the analytical results in Figure 4.3, where $\overline{D}$ denotes the average delay, However, the throughput performance of the ICA-based

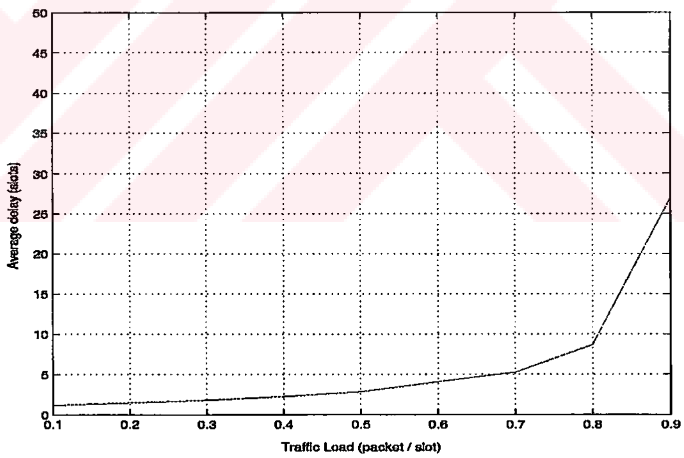

Figure 5.1. Average delay ($\overline{D}$) versus traffic load (λJ) for the ICA-based method when $SNR = \infty$ (single antenna)

method is slightly weaker than the analytical results in higher traffic loads, as shown in Figure 5.2. No error correction is applied to test ICA's resolution performance when there is no additive noise and collision multiplicity is always determined correctly.

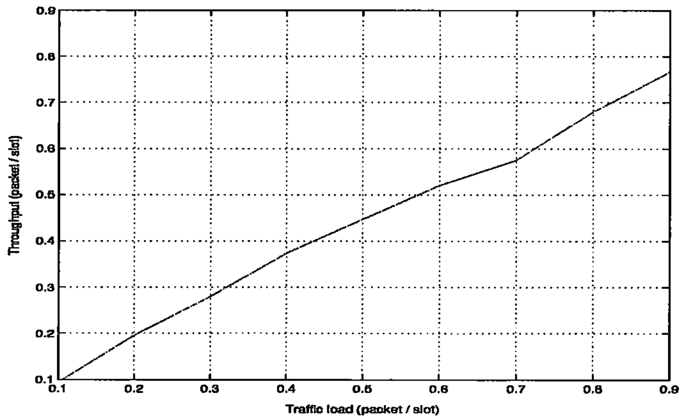

Figure 5.2. Throughput (λ_T) versus traffic load (λJ) for the ICA-based method when $SNR = \infty$ (single antenna)

Since the SNR is infinity, there is no possibility of underestimation errors for the collision multiplicity. Therefore, the only reason for the deterioration in throughput performance is the corrupted packets that are resolved with bit errors. Hence, ICA is more likely to produce bit errors as the number of packets involved in a collision increases.

The performance of the ICA-based collision resolution with AIC-based collision detection is tested under three SNR scenarios of 10, 15, and 20 dB.

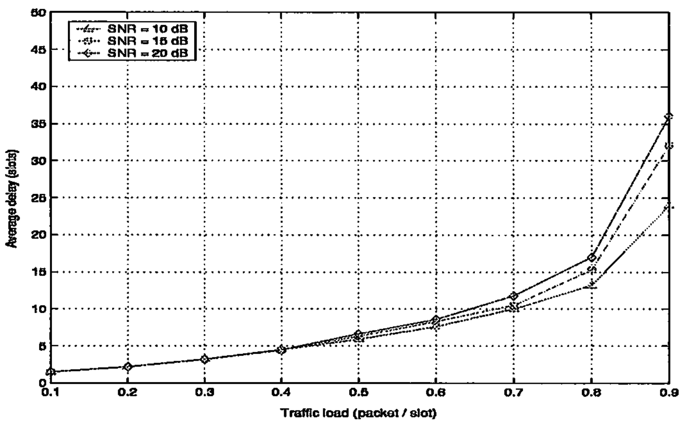

Figure 5.3. Average delay ($\overline{D}$) versus traffic load (λJ) for the ICA-based method (single antenna)

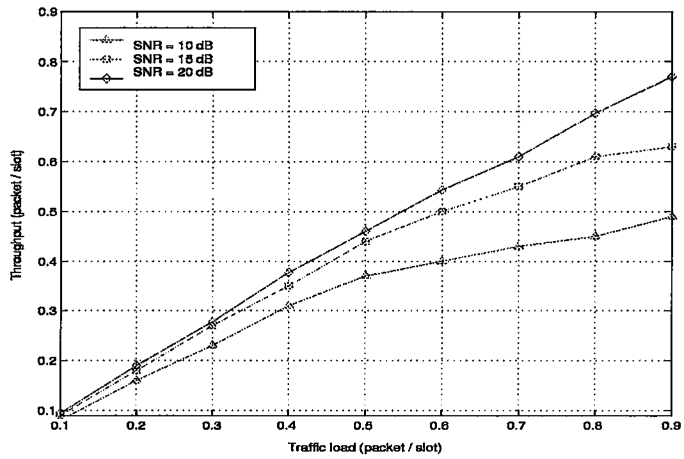

Figure 5.4. Throughput (λ_T) versus traffic load (λJ) for the ICA-based method with no error correction (single antenna)

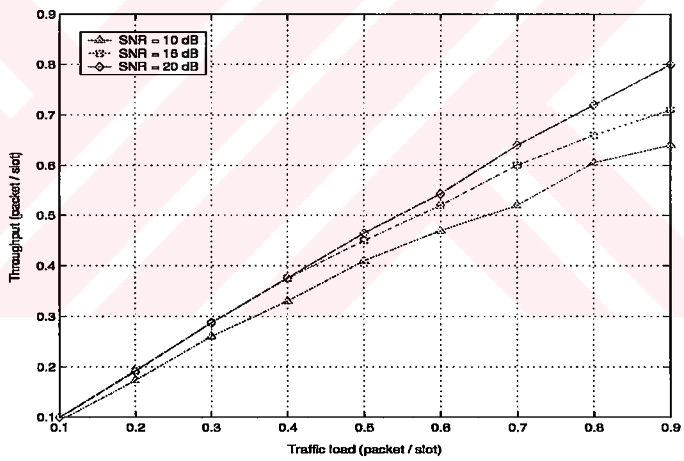

Figure 5.5. Throughput (λ_T) versus traffic load (λJ) for the ICA-based method with error correction (single antenna)

In the noiseless case, $K + 1$ number of transmissions is sufficient to determine the collision multiplicity K. This number is at least $K + 2$ for AIC if equation (4.8) is considered. In Figure 5.3, the average delay for SNR values of 15 and 20 dB are higher compared to the noiseless case in Figure 5.1, as expected. However, it is observed that the AIC method results in more underestimation errors as SNR decreases (especially for 10 dB SNR). Therefore the throughput performances in Figure 5.4 and 5.5 become weaker as the SNR reduces.

Besides, ICA results in more bit errors as SNR reduces, especially at high traffic loads. This is another factor which has a negative impact on the throughput performance. With error correction, the throughput performance improves as shown in Figure 5.5.

5.1.2. Throughput and Delay Performance in the Presence of Spatial Diversity

Simulation results are obtained under three SNR scenarios of 15, 20, and 25 dB. Average delay and throughput performances improve significantly compared to the single-antenna case as shown in Figure 5.6 and in Figures 5.7 and 5.8, respectively . Because of spatial diversity, the number of retransmissions reduces, and the average delay becomes less. Since fewer retransmissions are necessary, fewer packets wait in each user's packet buffer, lowering the collision multiplicity. Therefore, better throughput performance is observed because AIC results in fewer underestimations, and ICA is less likely to result in bit errors. When error correction is applied, the throughput performance increases.

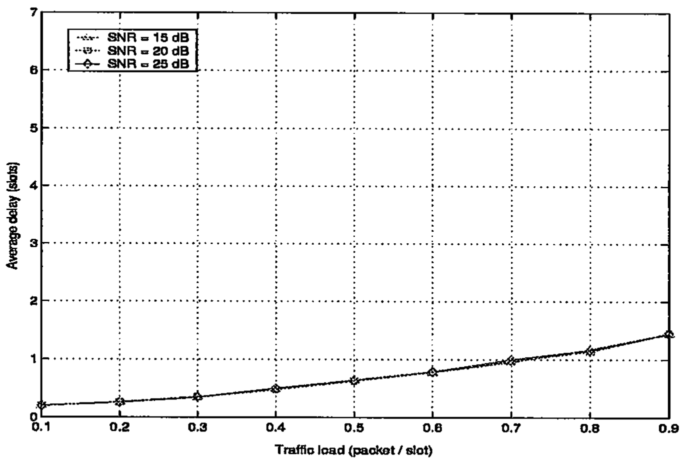

Figure 5.6. Average delay ($\overline{D}$) versus traffic load (λJ) for the ICA-based method (two antennas)

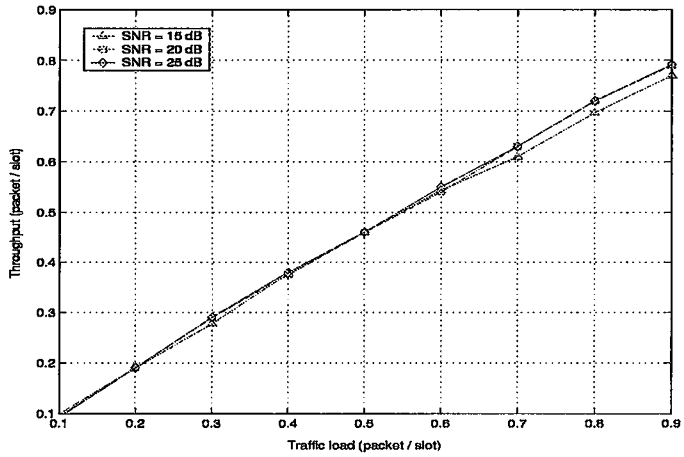

Figure 5.7. Throughput (λ_T) versus traffic load (λJ) for the ICA-based method with no error correction (two antennas)

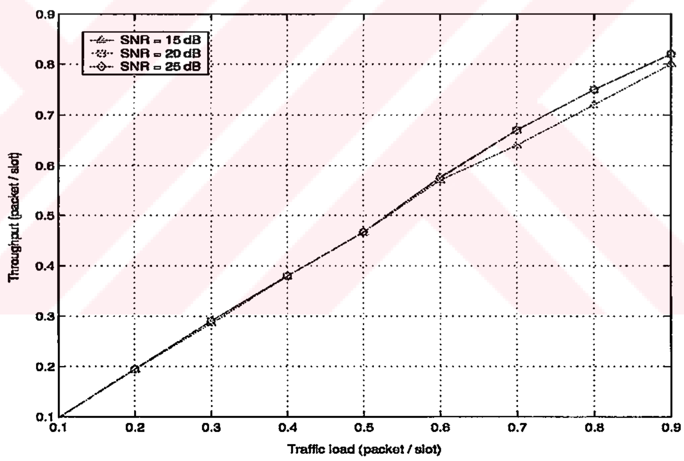

Figure 5.8. Throughput (λ_T) versus traffic load (λJ) for the ICA-based method with error correction (two antennas)

5.1.3. Delay Distributions

The delay for each packet, including the waiting time in the queue and transmission time in the channel, is found during simulations. For various SNR and traffic load scenarios, histograms of the packet delays are obtained to have an idea about the delay distribution of the system. The following figures show the distributions. The graph of a corresponding *Rayleigh* pdf [39, 37], which is shifted right by 2, is also fitted into each figure as a gray curve. The variable p in the figures denotes the Rayleigh distribution parameter for each pdf. Since AIC is used for the collision multiplicity detection, $K+2$ number of transmissions are required to resolve a K-packet collision. When there is no collision and only one packet is transmitted, three slots are necessary to detect the multiplicity. Thus, the minimum packet delay is two slots, and it is not possible to have a one-slot delay. This is the reason for the two-slot shift. When SNR is 10 dB and there is a single antenna at the base station, Figures 5.9, 5.10, and 5.11 show the delay distributions for traffic load values 0.1, 0.5, and 0.9 packet/slot, respectively.

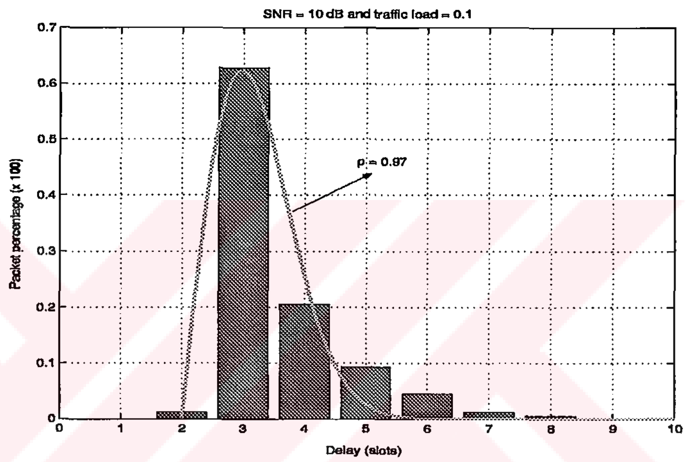

Figure 5.9. Delay distribution for the ICA-based method when SNR = 10 dB and traffic load (λJ) = 0.1 packet/slot (single antenna)

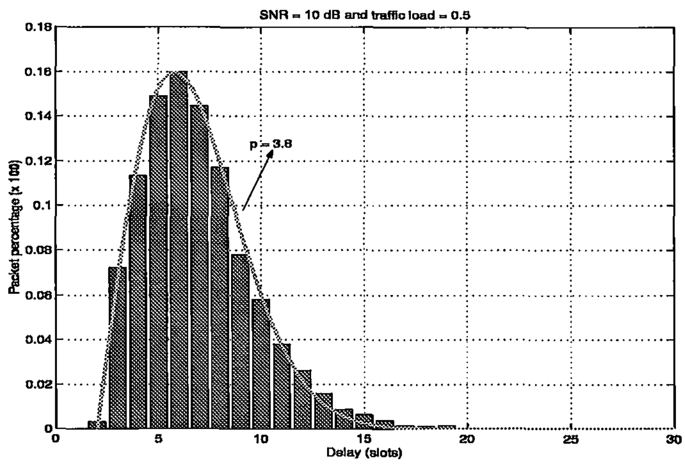

Figure 5.10. Delay distribution for the ICA-based method when SNR = 10 dB and traffic load (λJ) = 0.5 packet/slot (single antenna)

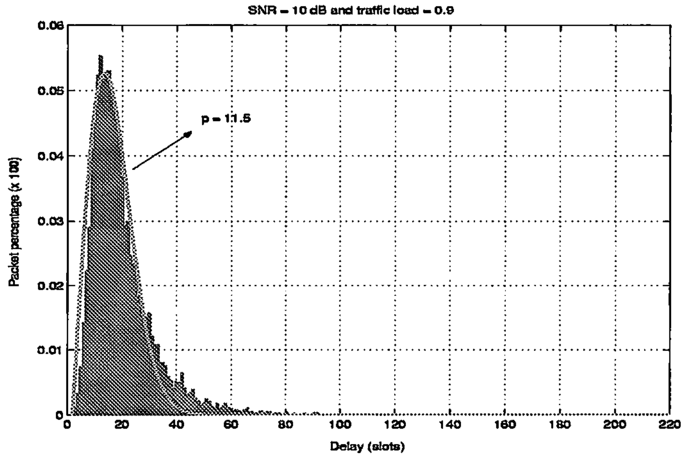

Figure 5.11. Delay distribution for the ICA-based method when SNR = 10 dB and traffic load (λJ) = 0.9 packet/slot (single antenna)

Figures 5.12, 5.13, and 5.14 illustrate the delay distributions in the single-antenna case for traffic load values 0.1, 0.5, and 0.9 packet/slot, respectively, when SNR is 15 dB.

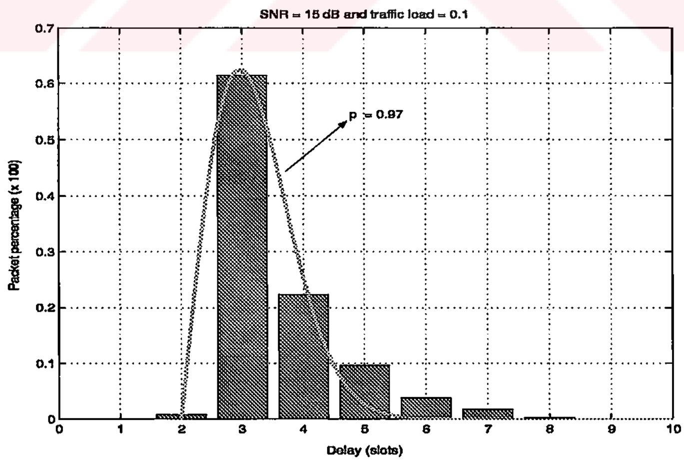

Figure 5.12. Delay distribution for the ICA-based method when SNR = 15 dB and traffic load (λJ) = 0.1 packet/slot (single antenna)

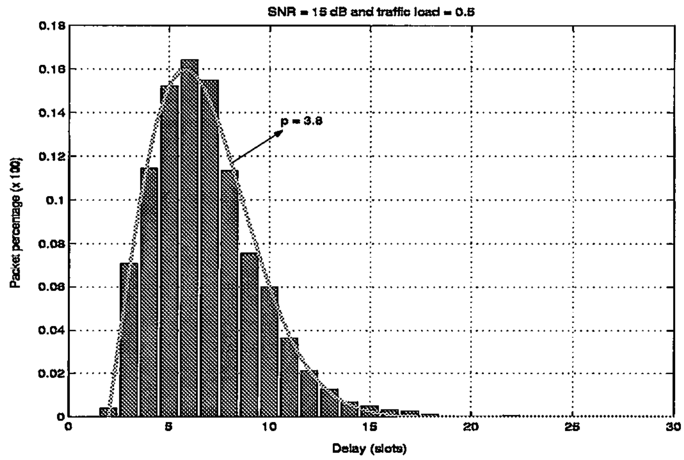

Figure 5.13. Delay distribution for the ICA-based method when SNR = 15 dB and traffic load (λJ) = 0.5 packet/slot (single antenna)

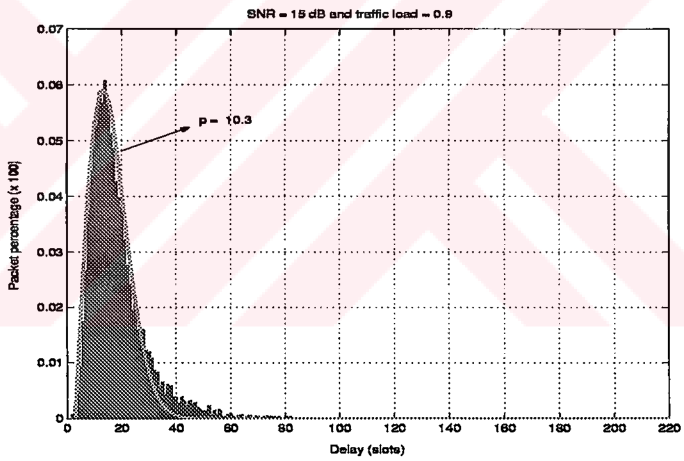

Figure 5.14. Delay distribution for the ICA-based method when SNR = 15 dB and traffic load (λJ) = 0.9 packet/slot (single antenna)

The delay distributions for the traffic load values 0.1, 0.5, and 0.9 packet/slot are shown in Figures 5.15, 5.16, and 5.17, respectively, when SNR is 20 dB and there is a single antenna at the BS.

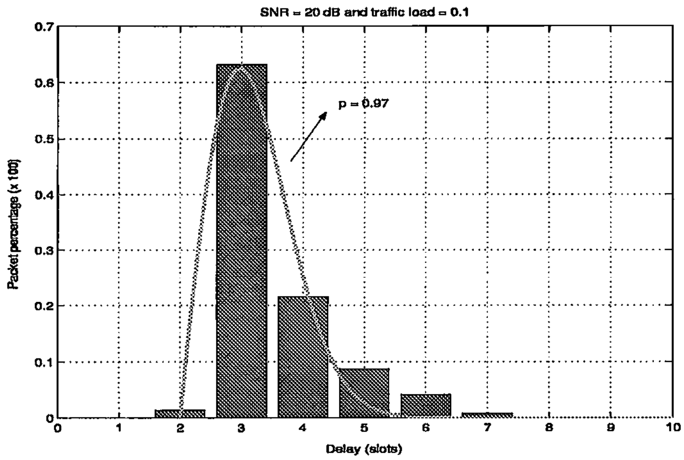

Figure 5.15. Delay distribution for the ICA-based method when SNR = 20 dB and traffic load (λJ) = 0.1 packet/slot (single antenna)

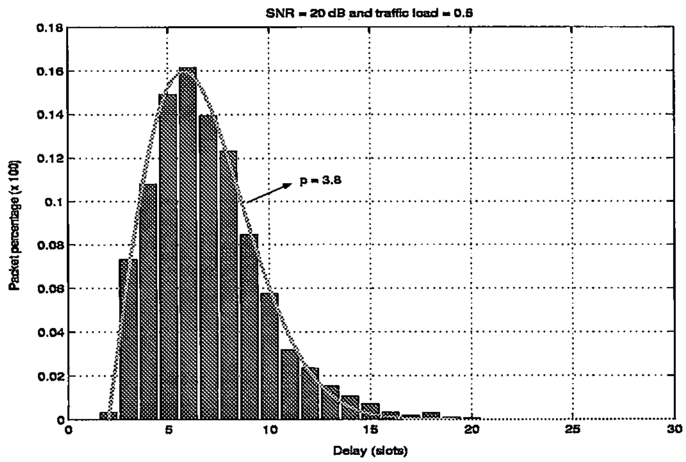

Figure 5.16. Delay distribution for the ICA-based method when SNR = 20 dB and traffic load (λJ) = 0.5 packet/slot (single antenna)

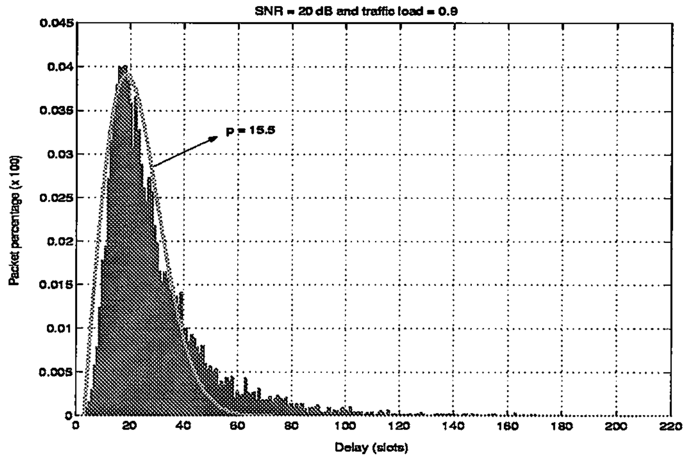

Figure 5.17. Delay distribution for the ICA-based method when SNR = 20 dB and traffic load (λJ) = 0.9 packet/slot (single antenna)

For all SNR scenarios, delay distributions spread more and resemble a Rayleigh distribution shifted right by 2 with increasing p as the traffic load increases. By modifying the Rayleigh pdf [33], the pdf $f_D(d)$ for the delay distribution is obtained as follows.

$$f_D(d) = \begin{cases} \frac{d-2}{p^2}\exp\{-\frac{(d-2)^2}{p^2}\}, & d \geq 2, \\ 0, & d < 2 \end{cases} \tag{5.1}$$

Even though the variance becomes larger as the traffic load increases, the packet delays are usually close to the mean. For instance, more than 80% of the packets have delays less than 40 channel slots when the traffic load is 0.9 packet/slot. In Figures 5.11, 5.14, and 5.17, there are a few packets spread al the way to the 200-slot range. However, they are not clearly visible in the figures.

5.2. The Comparison of the ICA-Based Multiple Access Method with NDMA and BNDMA

The major limitation of ICA is its statistical requirements on the collided packets. NDMA and BNDMA do not need these requirements such as the independence and non-Gaussian distribution of the packets. However, these assumptions are satisfied in practice. In this section, the performance of the ICA-based multiple access method is compared to NDMA and BNDMA depending on the theoretical information and the experimental results.

5.2.1. Comparison of the ICA-Based Multiple Access Method with NDMA

NDMA performs better than the ICA-based method and BNDMA in terms of throughput and delay performance [17, 18]. The reason is the orthogonal ID sequences which enable NDMA to detect the collision multiplicity and resolve the collision in fewer channel slots, resulting in higher throughput. However, the same orthogonal ID sequences result in a major drawback for NDMA. As the number of users in the system increases, the length of the ID sequences also increases linearly due to the orthogonality requirement. In large user populations, increasing the overhead reduces the available bandwidth necessary to transmit the packet payload. Therefore, blind schemes are desirable in practical implementation.

5.2.2. Comparison of the ICA-Based Multiple Access Method with BNDMA for the Single-Antenna Case

Figures 5.18 and 5.19 show the delay and throughput performance of BNDMA for the single-antenna case when the SNR is 10, 15, and 20 dB. The necessary data for these figures are obtained from the simulation results in [19] for traffic load values, $\lambda J = 0.1n$ where $n = 1, 2, \ldots, 9$. The number of users in the system is $J = 16$. Fading channel is constant during the collision resolution epochs, and no error correction is done. SNR is regarded as the signal power of one packet over the noise power, and average SNR is not taken into account.

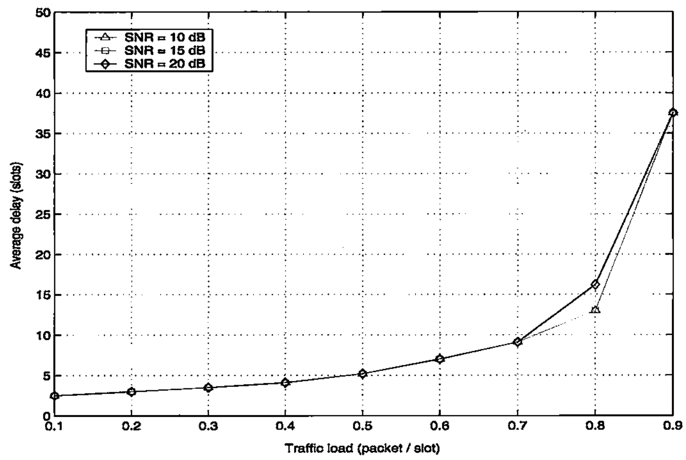

Figure 5.18. Average delay ($\overline{D}$) versus traffic load (λJ) for BNDMA (single antenna)

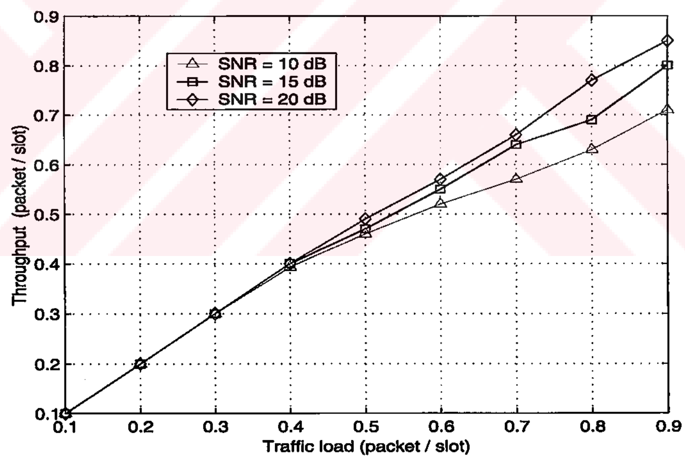

Figure 5.19. Throughput (λ_T) versus traffic load (λJ) for BNDMA (single antenna)

The average delay performance of the ICA-based method in Figure 5.3 (which uses AIC for blind collision detection) is better than that of BNDMA in Figure 5.18 (which uses rank test method for blind the collision detection). However, this is not an advantage because compared to the analytical results in Figure 5.1, AIC results in underestimation errors when SNR decreases and traffic load is high (such as the 10 dB case in Figure 5.18), which also has a negative impact on the throughput performance of the ICA-based method.

Since the rank test method uses a threshold which can be adjusted depending on the noise power, the average delay performances for different SNRs in Figure 5.18 are close to each other. However, if the threshold is not chosen properly, underestimation/overestimation errors may occur. As an example, the rank test method needs $K + 1$ transmissions to resolve a K-fold collision, whereas AIC needs $K + 2$ transmissions, as long as there is no underestimation/overestimation. However, the average delay obtained by using the rank test method in Figure 5.18 is higher than that of the AIC-based collision detection in Figure 5.3 and analytical results in Figure 4.3, which points to the overestimation. It is also hard to decide on a proper threshold in fast-fading channels, which is the case for the signaling model in (2.1).

When no error correction is applied in our simulations after ICA-based collision resolution, there is no significant difference between the throughput performance of the ICA-based method in Figure 5.4 and BNDMA method in Figure 5.19. The marginally worse throughput of ICA-based multiple access in noisy channels stems in part from the extra slot required by the AIC-based collision detector. It is also important to point out that fading is constant during the collision resolution epoch and the mixing matrix is controlled to have a Vandermode structure in BNDMA simulations [19]. Throughput performance of the ICA-based method is improved by applying error correction as shown in Figure 5.5.

Finally, the signaling model for ICA-based method does not require the phase control of transmitted packets, as shown in (2.4), and the fading process can be faster than what BNDMA requires, since the fading coefficients $f_m(r, k)$ in (2.5) change in every retransmission slot during the collision resolution epoch. In addition, the ICA-based method does not need the antenna gains $g_m(r, k)$ in (2.4) to be constant during the collision resolution epoch as BNDMA does.

5.2.3. Comparison of the ICA-Based Multiple Access Method with BNDMA in the Presence of Spatial Diversity

Figures 5.20 and 5.21 show the delay and throughput performance of BNDMA method with two antennas at the BS when the SNR is 15, 20, and 25 dB. The necessary data for these figures are from the simulations in [18] for traffic load values, $\lambda J = 0.1n$ where $n = 1, 2, \ldots, 8$. The number of users in the system is again $J = 16$. The superiority of the ICA-based method reveals itself when spatial diversity is applied at the BS. As mentioned previously, the number of transmissions that ICA needs for the collision resolution is $\lceil K/M \rceil$. The number of transmissions required by PARAFAC is given in (2.8). By comparing these two expressions, more transmissions are necessary for BNDMA as the number of collided users increases (and the traffic load becomes larger). Therefore, in larger populations, the performance of ICA is expected to be much better in high traffic loads.

Simulation results are also consistent with the above description. Delay performance of the ICA-based method in Figure 5.6 is better than the BNDMA performance in Figure 5.20 in case of high traffic load. Since the collision multiplicity decreases in the presence of spatial diversity, throughput performance of ICA-based method is also improved as shown in Figure 5.7, which is very close to the throughput performance of BNDMA in Figure 5.21. When error correction is applied, throughput performance of ICA-based method improves further as shown in Figure 5.8.

Contrary to BDNMA, the ICA-based method does not require the antenna gains $g_m(r, k)$ in (2.4) to be constant throughout the resolution epoch.

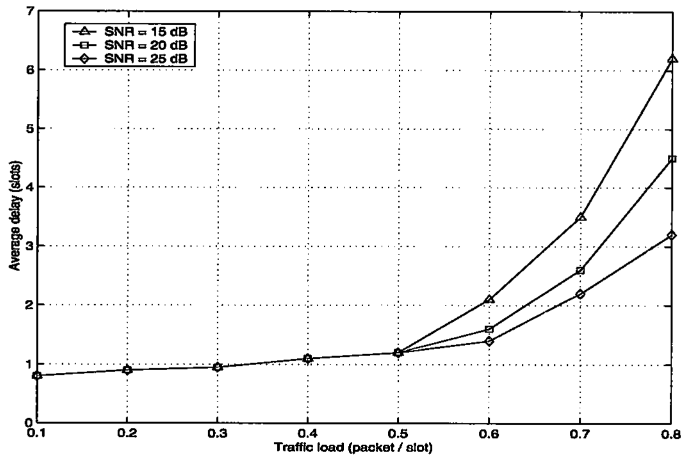

Figure 5.20. Average delay ($\overline{D}$) versus traffic load (λJ) for BNDMA (two antennas)

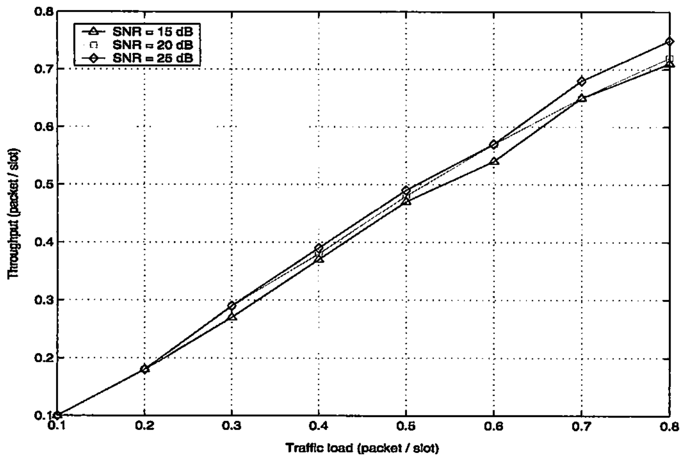

Figure 5.21. Throughput (λ_T) versus traffic load (λJ) for BNDMA (two antennas)

6. CONCLUSIONS

In this thesis, an entirely blind multiple access method is proposed for the retransmission scheduling, collision detection, and the collision resolution. Collision detection is accomplished by using AIC, and packet collisions are resolved via ICA.

ICA is more likely to result in bit errors as the SNR reduces and the collision multiplicity increases. Therefore, ICA-based multiple access method has a weaker throughput performance at lower SNR values and higher traffic loads. Throughput performance can be improved by applying error correction after collision resolution.

Performance of the collision detector has a considerable impact on the system throughput and transmission delay. If the collision multiplicity is underestimated by the collision detector, ICA is not able to resolve all the collided packets, and throughput performance suffers. In case of overestimation, extra channel slots are wasted during retransmissions and delay performance suffers this time. AIC generally has a good performance for detecting the collision multiplicity. However, it results in underestimation errors at high traffic loads as the SNR decreases. Rank test method, described in Section 4.2, has the advantage of choosing a tolerance threshold for different SNR scenarios, but it is hard to determine a proper threshold in fast fading channels, which makes AIC more implementable and reliable.

NDMA is the multiple access technique with better throughput and delay performance compared to ICA-based method [17, 18]. However, a direct performance comparison is not fair since NDMA needs unique, user-specific, and mutually-orthogonal ID sequences to be inserted as a prefix to the packets of the users. In larger populations, this property results in an increased overhead, proportionally reducing the bandwidth for carrying the packet payload.

BNDMA is another blind multiple access technique which employs PARAFAC analysis for the collision resolution [18, 19]. ICA-based method has several advantages compared to BNDMA. In the single-antenna case, BNDMA requires

- tight control of the transmitter phase;
- a fading process slow enough to be constant during the transmissions for collision resolution;
- constant antenna gains for each user during the transmissions for collision resolution.

None of the above restrictions are necessary for the ICA-based method according to the signaling model established in Chapter 2.

In the presence of spatial diversity, ICA requires fewer transmissions compared to PARAFAC [18]. Therefore, ICA-based method has better delay performance especially at higher traffic loads and in larger populations compared to BNDMA. Besides, BNDMA needs the antenna gains of each user to be constant during the transmissions for collision resolution, which is not a requirement for ICA-based method.

As a result, ICA is an efficient collision resolution technique in fast flat fading channels. However, the statistical requirements and distribution-dependent algorithm of ICA are the drawbacks compared to other proposed methods. Moreover, there is no proper ICA algorithm which can be employed for the complex-valued independent signals in the presence of additive noise. That is why the collision resolution technique in this thesis is only employed for BPSK constellation and the frequency selective fading channel is not taken into account. However, there are some ongoing studies about ICA algorithms for complex-valued signals [28]. Depending on further improvements of these algorithms which also take additive Gaussian noise into account, ICA-based method can be employed for the collision resolution of complex-valued constellations, and can also be used in frequency dispersive channels (as it is done for NDMA in [40]) in the future.

REFERENCES

1. Rappaport, T. S., *Wireless Communications, Principles and Practice*, Prentice Hall, Upper Saddle River, NJ, 1996.

2. TIA IS-95A, *Mobile Station-Base Station Compatibility Standard for Dual-Mode Wideband Spread Spectrum Cellular System*, March 1995.

3. Bertsekas, D. and R. Gallager, *Data Networks, Second Edition*, Prentice Hall, Englewood Cliffs, NJ, 1992.

4. Zorzi, M. and L. Tomba, "A Comparison of CDMA, TDMA, and Slotted ALOHA Multiple Access Schemes in Cellular Mobile Radio Systems", *PIMRC'94 Conference*, Netherlands, September 1994, pp. 776-780.

5. Frullone. M., G. Riva, P. Grazioso, and M. Missiroli, "Comparisions of Multiple Access Schemes for Personal Communication Systems in a Mixed Cellular Environment", *IEEE Transactions on Vehicular Technology*, vol. 43, no. 1, pp. 99-109, February 1994.

6. Abramson, N.,"The Aloha System - Another Alternative for Computer Communications", *AFIPS Conference Proceedings*, vol. 36, 1970, pp. 295-298.

7. Capetanakis, J. I., "Tree Algorithms for Packet Broadcast Channels", *IEEE Transactions on Information Theory*, vol. 25, pp. 505-515, 1979.

8. Hayes, J. F., "An Adaptive Technique for Local Distribution", *IEEE Transactions on Communications*, vol. 26, pp. 1476-1484, 1978.

9. Paterakis, M. and P. Papantoni-Kazakos, "A Simple Window Random Access Algorithm with Adventageous Properties", *IEEE Transactions on Information Theory*, vol. 35, pp. 1124-1130, 1989.

10. Tsybakov, B. S. and V. A. Mikhailov, "Slotted Multiaccess Packet Broadcasting Feedback Channel", *Problemi Peredachi Informatsii*, vol. 14, 1978.

11. Tsybakov, B. S. and V. A. Mikhailov, "Packet random multiple access: part-and-try algorithm", *Problemi Peredachi Informatsii*, vol. 16, pp. 65-79, 1980.

12. Mikhailov, V. A and B. S. Tsybakov, "Upper Bound for the Capacity of a Random Multiple Access System", *Problemi Peredachi Informatsii*, vol. 17, pp. 90-95, 1981.

13. Zorzi, M., "Mobile Radio Slotted ALOHA with Capture and Diversity", *Wireless Networks*, vol. 1, pp. 227-239, May 1995.

14. Zorzi, M., "Mobile Radio Slotted ALOHA with Capture, Diversity, and Retransmission Control in the Presence of Shadowing", *Wireless Networks*, vol. 4, pp. 379-388, August 1998.

15. Lyons, D. F. and P. Papantoni-Kazakos, "A Window Random Access Algorithm for Environments with Capture", *IEEE Transactions on Communications*, vol. 37, pp. 766-770, July 1989.

16. Yücel, B. and H. Deliç, "Mobile Radio Window Random-Access Algorithm with Diversity", *IEEE Transactions on Vehicular Technology*, vol. 49, pp. 2060-2070, November 2000.

17. Tsatsanis, M. K., R. Zhang, and S. Banerjee, "Network-Assisted Diversity for Random Access Wireless Networks", *IEEE Transactions on Signal Processing*, vol. 48, no. 3, pp. 702-711, March 2000.

18. Tsatsanis, M. K., R. Zhang, and N. D. Sidiropoulos, "Performance Analysis of a Random Access Packet Radio System with Joint Network-Spatial diversity", *Proceedings of the IEEE International Conference on Acoustics, Speech and Signal Processing*, Istanbul, Turkey, June 2000, pp. 2593-2596.

19. Zhang, R., N. D. Sidiropoulos, and M. K. Tsatsanis, "Collision Resolution in Packet

Radio Networks Using Rotational Invariance Techniques", *IEEE Transactions on Communications*, vol. 50, no. 1, pp. 146-155, January 2002.

20. Sidiropoulos, N. D., G. B. Giannakis, and R. Bro, "Blind PARAFAC Receivers for DS-CDMA Receivers", *IEEE Transactions on Signal Processing*, vol. 48, no. 3, pp. 810-823, March 2000.

21. Sidiropoulos, N. D., R. Bro, and G. B. Giannakis, "Parallel Factor Analysis in Sensor Array Processing", *IEEE Transactions on Signal Processing*, vol. 48, no. 8, pp. 2377-2388, August 2000.

22. Bro, R., N. D. Sidiropoulos, and G. B. Giannakis, "Optimal Joint Azimuth-Elevation and Signal-Array Response Estimation Using Parallel Factor Analysis", *Proceedings on 32nd Asilomar Conference on Signals, Systems, and Computers*, November 1998, Monterey, CA.

23. Hyvärinen, A. and E. Oja, "Independent Component Analysis: Algorithm and Application", *Neural Networks*, vol. 13(4-5), pp. 411-430, June 2000.

24. Comon, P., "Independent Component Analysis - A New Concept?", *Signal Processing*, vol. 36, pp. 287-314, 1994.

25. Hyvärinen, A., "Fast and Robust Fixed-Point Algorithms for Independent Component Analysis", *IEEE Transactions on Neural Networks*, vol. 10, no. 3, pp. 626-634, May 1999.

26. Hyvärinen, A. and E. Oja, "A Fast Fixed-Point Algorithm for Independent Component Analysis", *Neural Computation*, vol.9, no. 7, pp. 301-313, 1998.

27. Hyvärinen, A., "Independent Component Analysis in the Presence of Gaussian Noise by Maximizing Joint Likelihood", *Neurocomputing*, vol. 22, no. 1-3, pp. 49-67, October 1998.

28. Bingham, E. and A. Hyvärinen, "A Fast Fixed Point Algorithm for Independent

Component Analysis of Complex-Valued Signals", *International Journal of Neural Systems*, vol. 10, no. 1, pp. 1-8, February 2000.

29. Ristaniemi, T. and J. Joutsensalo, "On the Performance of Blind Source Separation in CDMA Downlink", *Proceedings of the International Workshop on Independent Component Analysis and Signal Separation*, Aussois, France, pp. 437-442, January 1999.

30. Ristaniemi, T. and J. Joutsensalo, "Independent Component Analysis with Code Information Utilization in CDMA Signal Separation", *Proceedings of the IEEE GLOBECOM*, vol. 1a, Rio de Janeiro, Brasil, December 1999, pp. 320-324.

31. Ristaniemi, T. and J. Joutsensalo, "Advanced ICA-Based Receivers for DS-CDMA Systems", *Proceedings of the 11th IEEE Symposium on Personal, Indoor and Mobile Radio Communications*, London, England, September 2000, pp. 276-281.

32. Karhunen, J., A. Hyvärinen, R. Viagrio, J Hurri, and E. Oja, "Applications of Neural Blind Separation to Signal and Image Processing", *Proceedings of IEEE International Conference on Acoustics, Speech and Signal Processing (ICASSP'97)*, pp. 131-134, Munich, Germany, 1997.

33. Haykin, S., *Communication Systems, Third Edition*, John Wiley and Sons, NY, 1994.

34. Wax, M. and T. Kailath, "Detection of Signals by Information Theoretic Criteria", *IEEE Transactions on Acoustic Speech Signal Processing*, vol. ASSP-33, pp. 387-392, April 1985.

35. Liavas, A. P. and P. A. Regalia, "On the Behaviour of Information Theoretic Criteria for Model Order Selection", *IEEE Transactions on Signal Processing*, vol. 49, pp. 1689-1695, August 2001.

36. Kleinrock, L., *Queueing Systems*, vol. 1, John Wiley and Son, NY, 1975.

37. Drake, A. W., *Fundamentals of Applied Probability Theory*, McGraw-Hill, NY, 1967.

38. Wilson, S. G., *Digital Modulation and Coding*, Prentice Hall, Upper Saddle River, NJ, 1996.

39. Shanmugan, K. S. and A. M. Breipohl, *Random Signals: Detection, Estimation and Analysis*, John Wiley and Sons, NY, 1988.

40. Zhang, R. and M. K. Tsatsanis, "Network-Assisted Diversity Multiple Access in Dispersive Channels", *IEEE Transactions on Communications*, vol. 5, pp. 623-632, April 2002.